

Outline of Dendrites Lecture

Basic Properties of Synaptic Currents

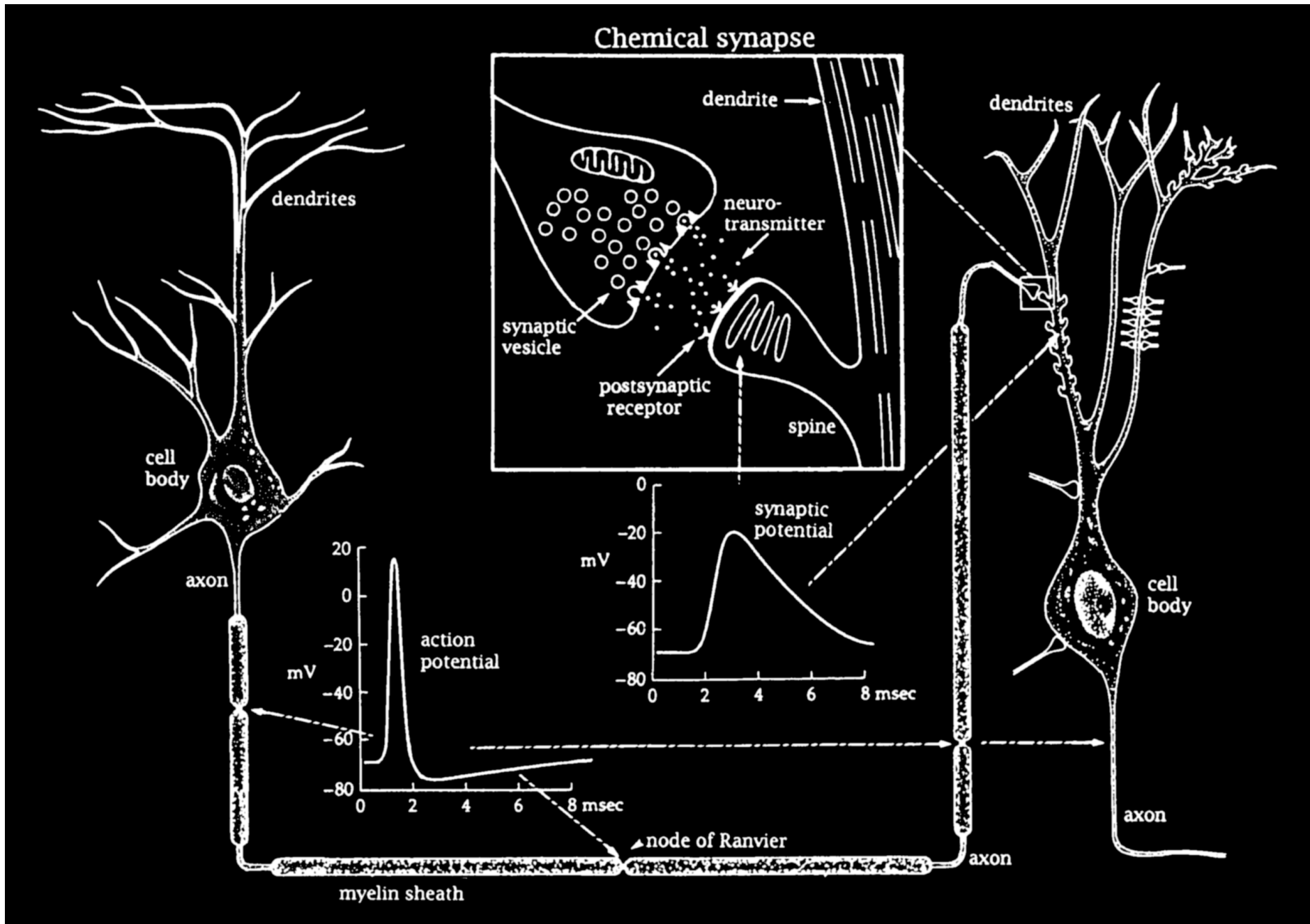
Morphology of Dendrites

Passive Cable Properties - Rall Model

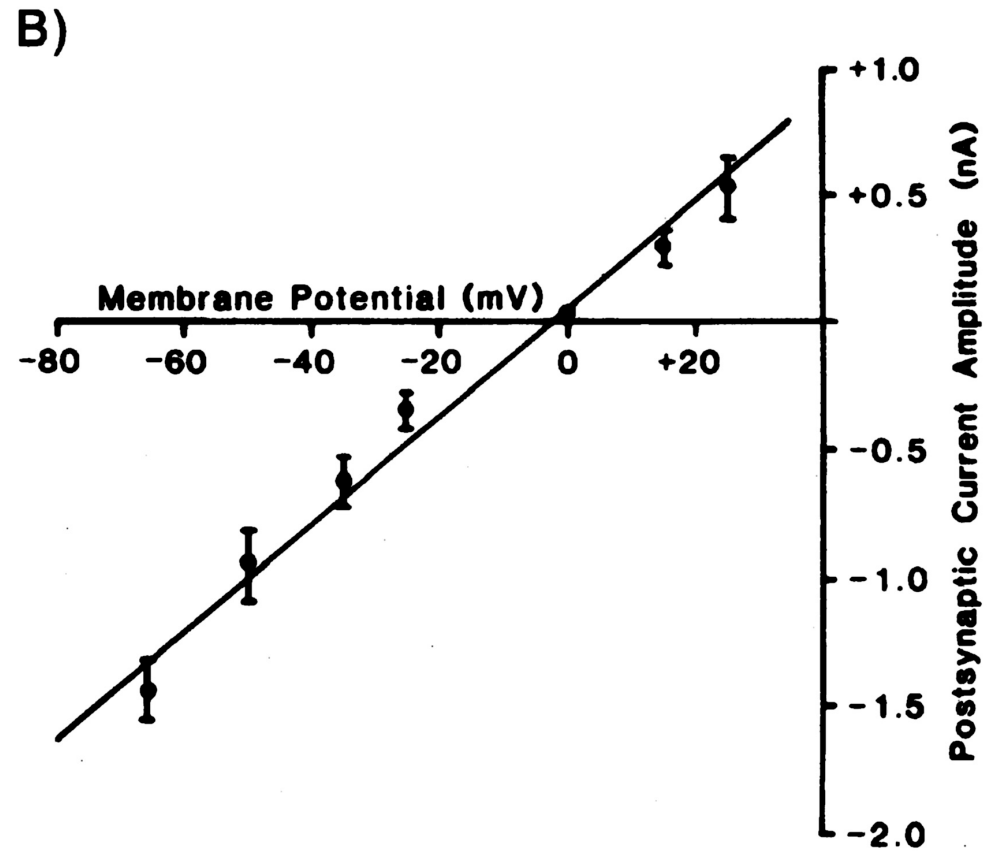
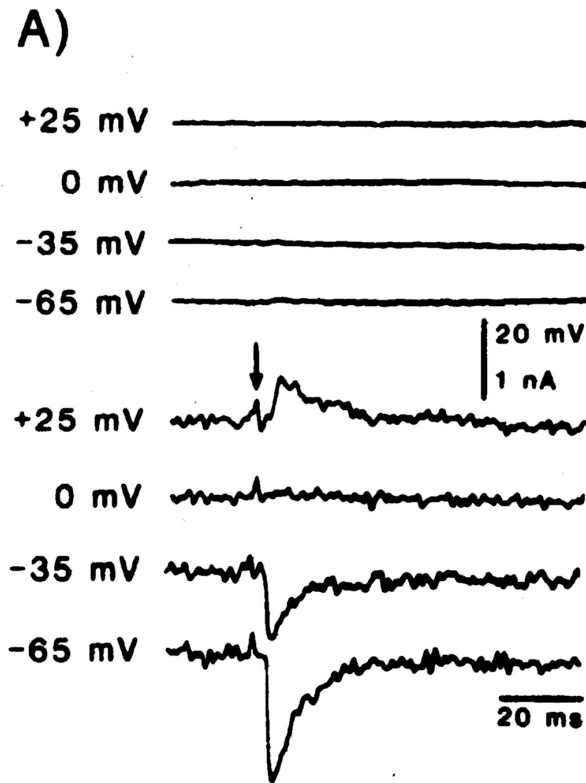
Measuring and Modeling PSP Attenuation and Summation

Active Dendrites

Computation in Dendrites



Membrane Conductance Change Underlying a Synaptic Potential
voltage clamp of synaptic current



Augment generalized H/H equations
with synaptic conductance terms:

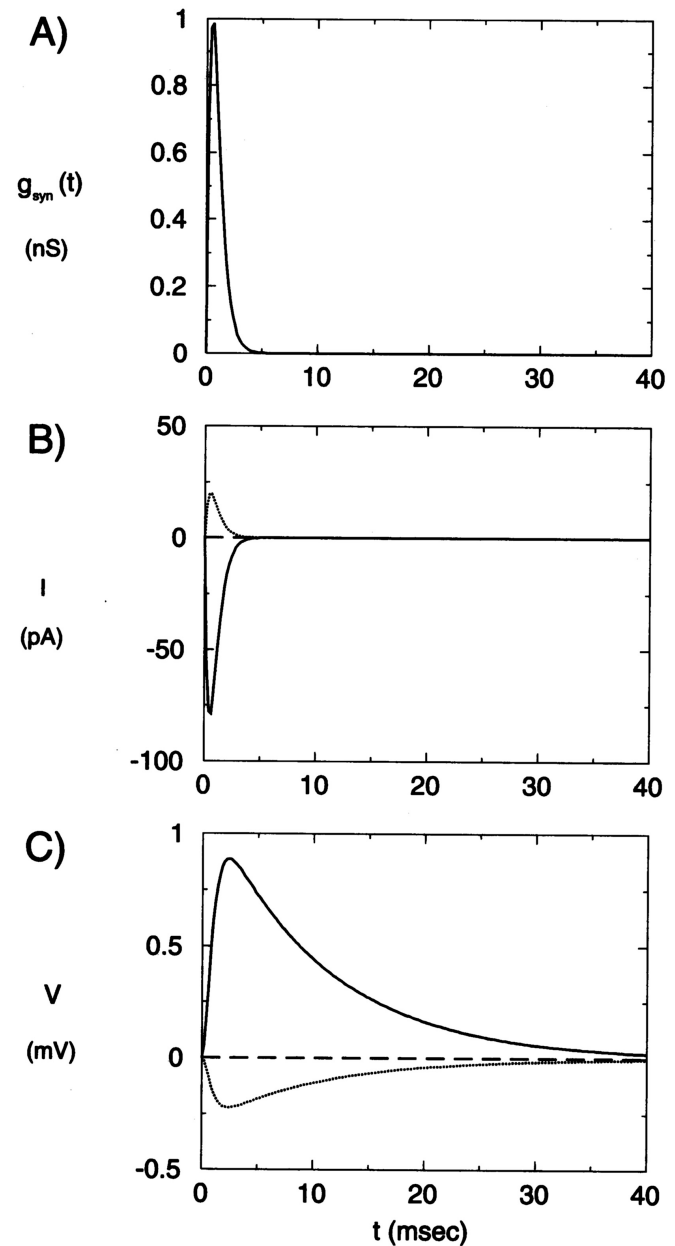
$$I_{syn} = g_{syn}(t)(V_m - V_{syn})$$

a function

$$g_{syn}(t) = \bar{g}_{syn} t e^{-t/t_{peak}}$$

or difference of two exponentials

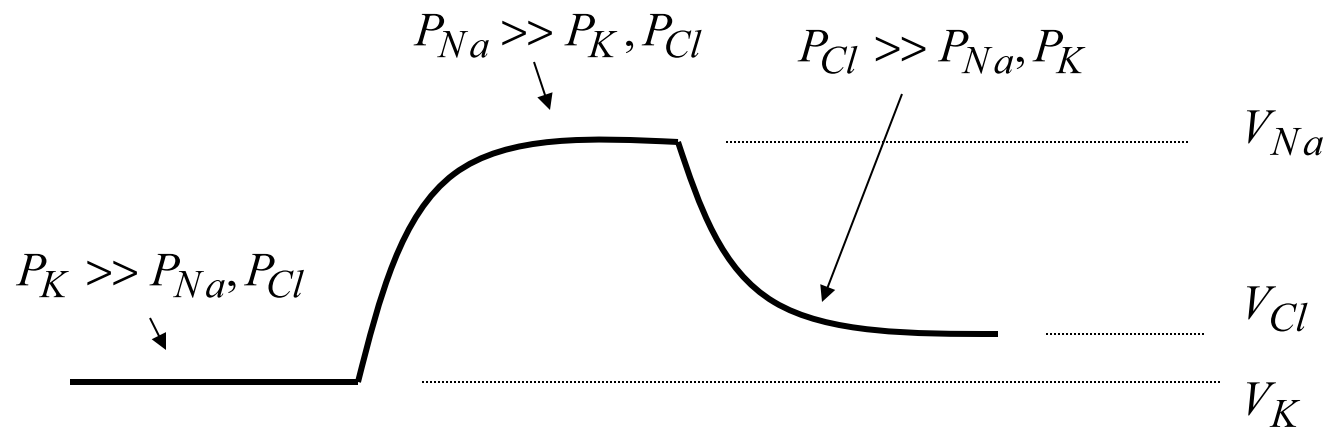
$$g_{syn}(t) = \bar{g}_{syn} (e^{-t/\tau_1} - e^{-t/\tau_2})$$



Goldman Hodgkin Katz Equation

$$V = 58 \log \frac{P_K [K]_{ext} + P_{Na} [Na]_{ext} + P_{Cl} [Cl]_{int}}{P_K [K]_{int} + P_{Na} [Na]_{int} + P_{Cl} [Cl]_{ext}}$$

$P_K : P_{Na} : P_{Cl}$ relative permeabilities



“inhibitory/hyperpolarizing” →

“Excitatory/depolarizing” →

“inhibitory/shunting” →

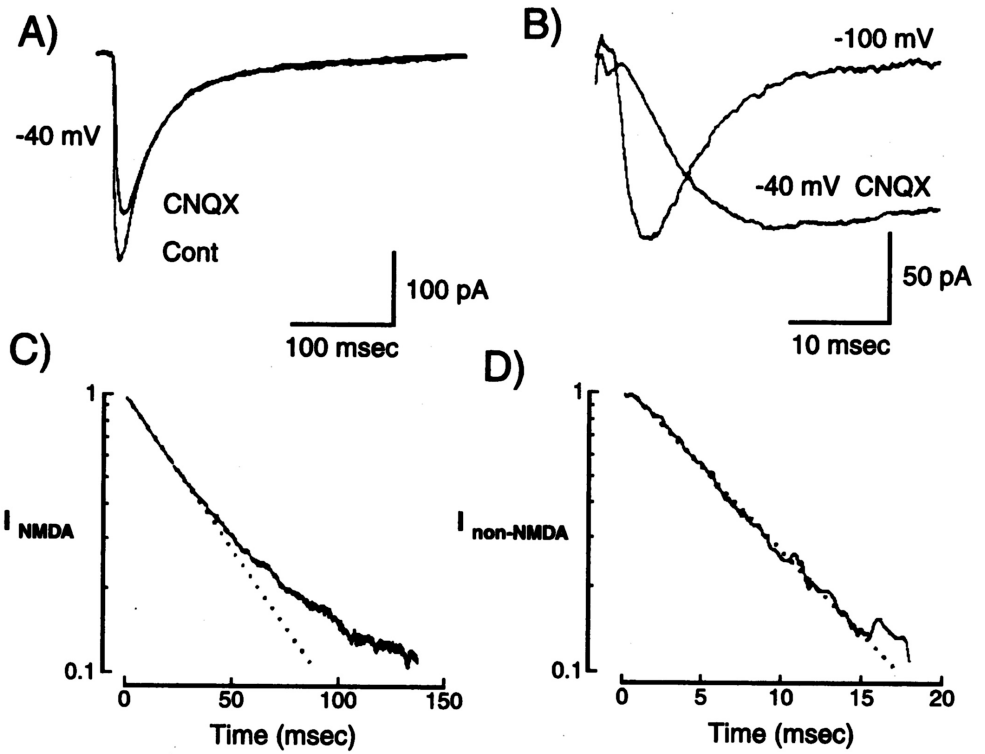
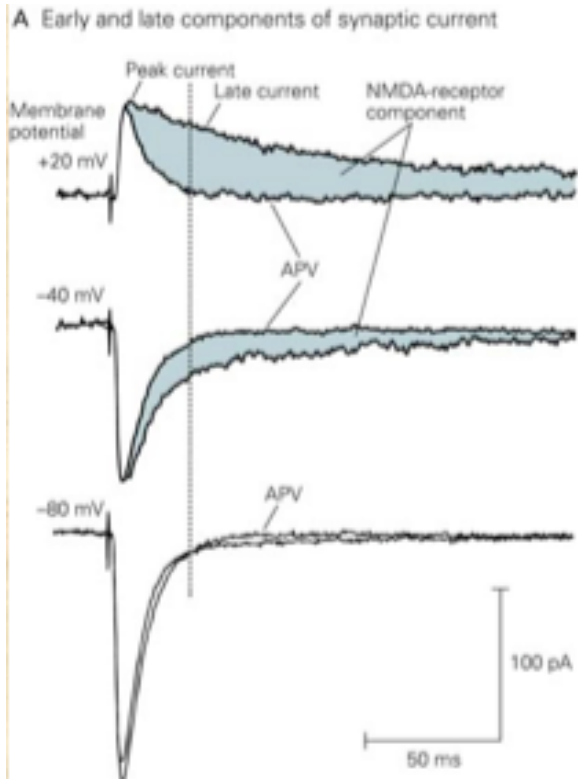
	[out]	[in]	E	P/PK
	(mM)	(mM)	(mV)	
K ⁺	5	100	-80	1
Na ⁺	150	15	+62	0.025
Ca ²⁺	2	0.0002	+123	–
Cl ⁻	150	13	-65	0.1

GABA_BR

GABA_AR, GlyR

$$V_m = -65 \text{ mV}$$

AMPA and NMDA currents



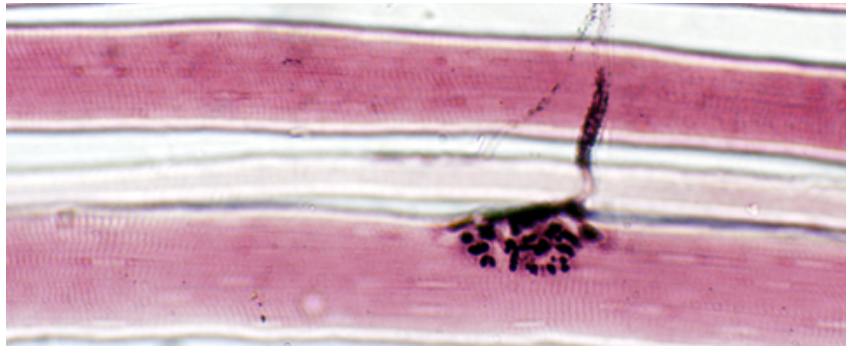
Voltage dependent activation of NMDA component



V_{thr}

V_{rest}

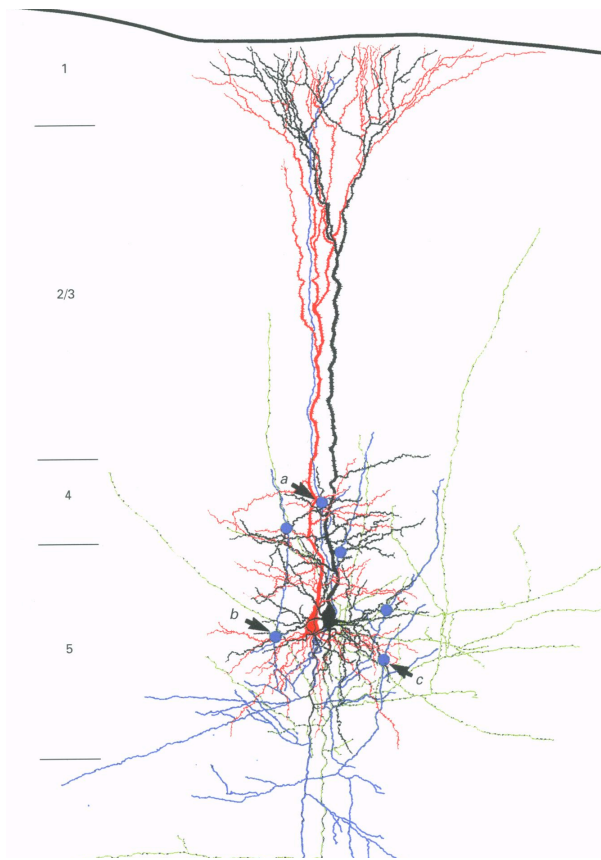
Synaptic input required to generate an AP



Neuromuscular Junction

- Many tens of synaptic boutons per axon
- Many release sites per bouton

EJPs from the input from a single motoneuron are large

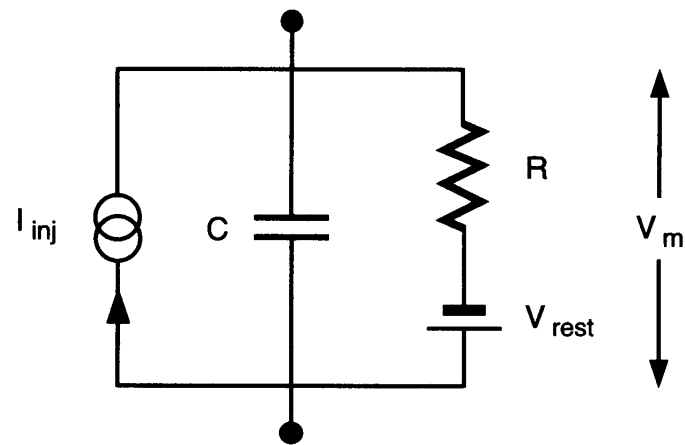
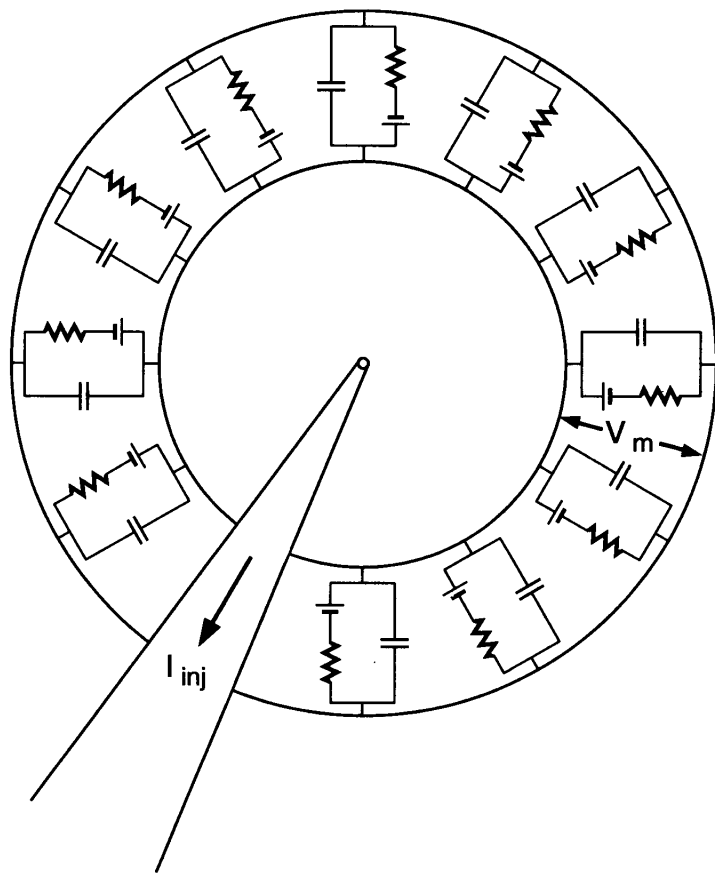


Central Synapses

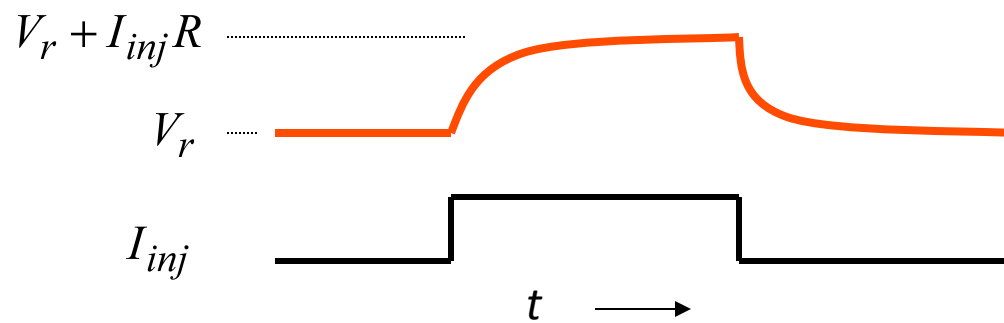
- The axon from a given presynaptic cell only has a few (1-5) synaptic boutons onto a given postsynaptic target cell
- Typically only one release site per bouton
- Very small quantal size

EPSPs from single presynaptic cells are small (0.1mV)
Summation of many presynaptic cells required for AP generation

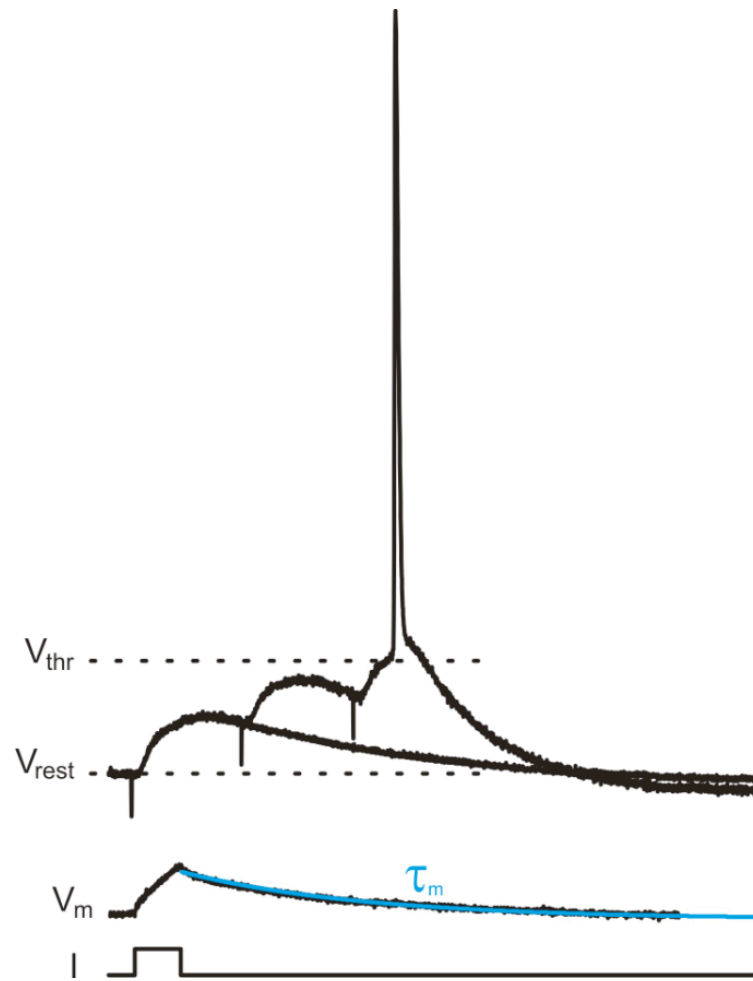
Markram et al., J. Physiol. (1997)



$$C \frac{dV_m}{dt} = I_{inj} + \frac{V_m - V_r}{R}$$

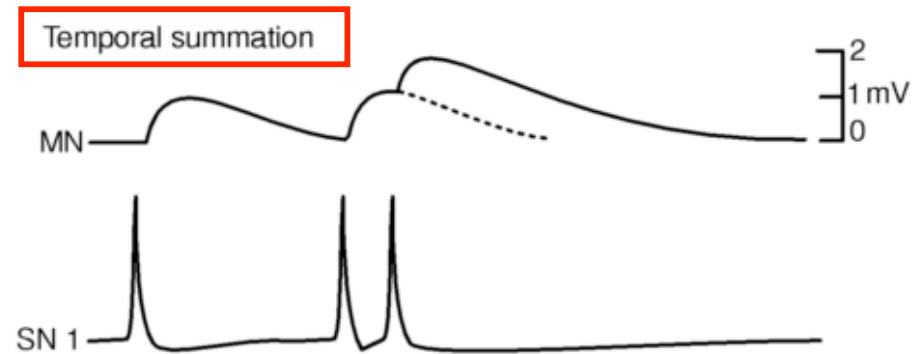
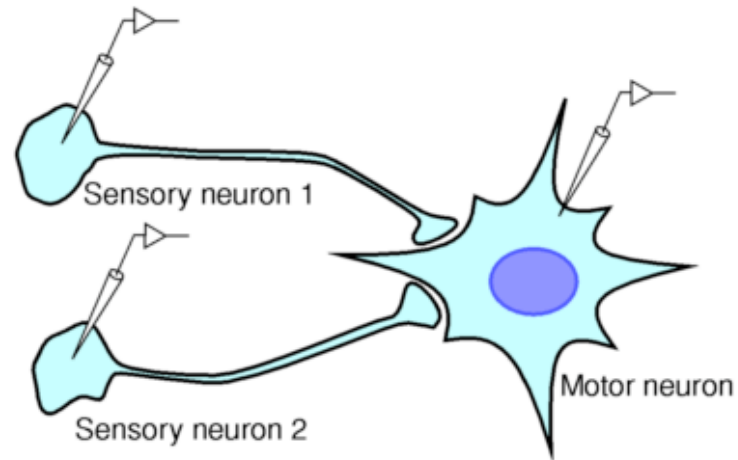


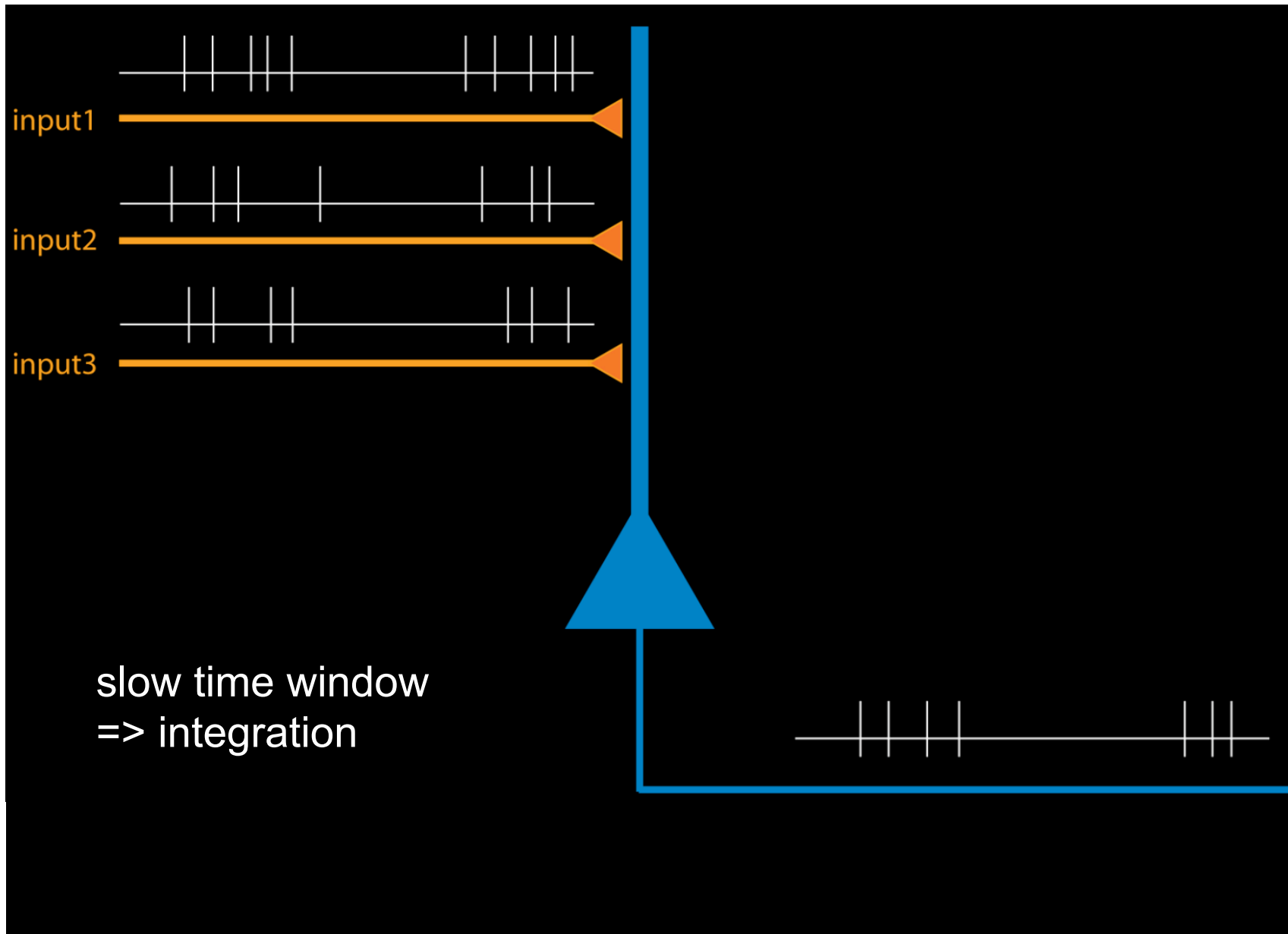
Membrane Time Constant Sets the Scale of Temporal Summation

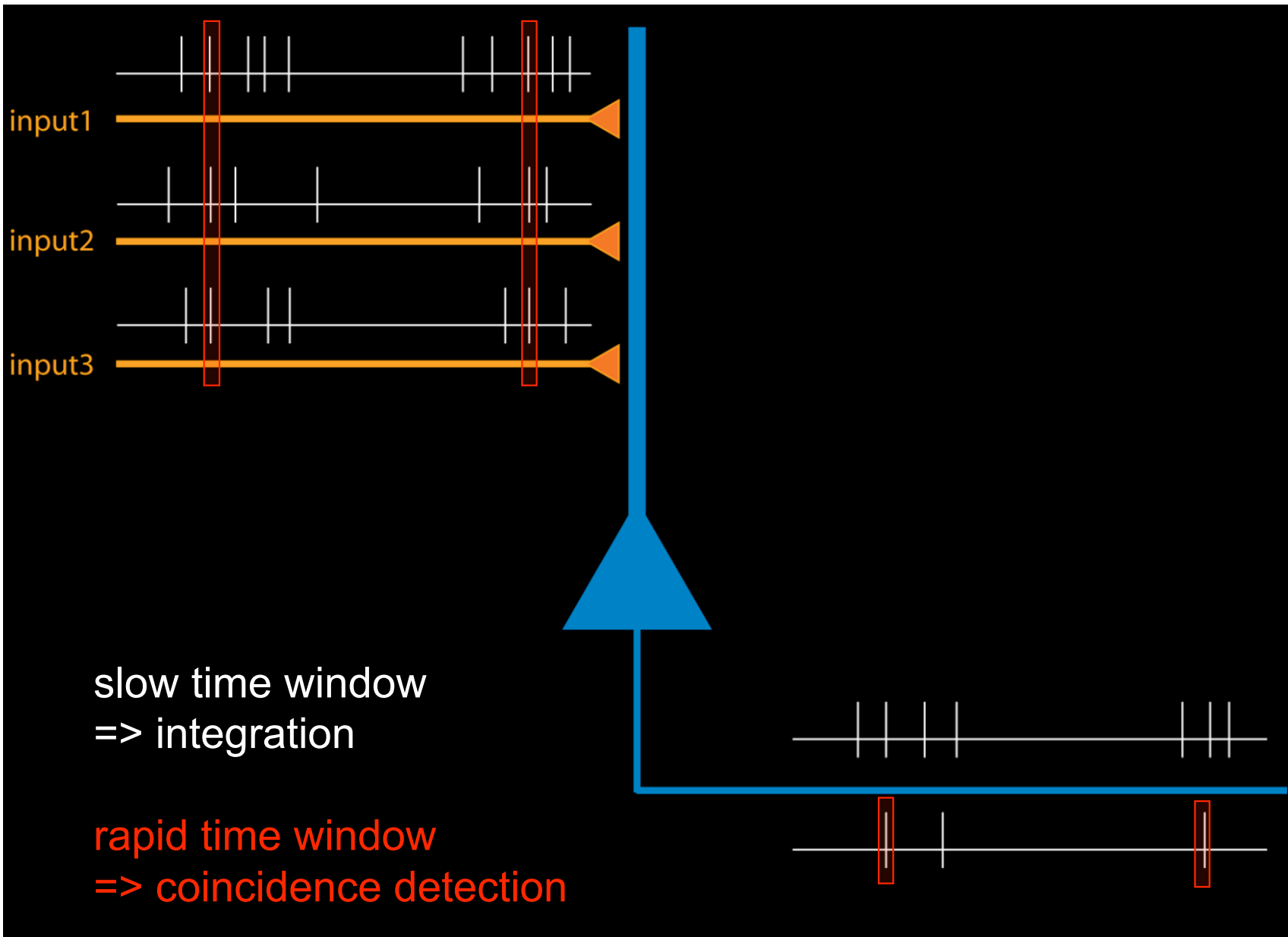


M. Scanziani

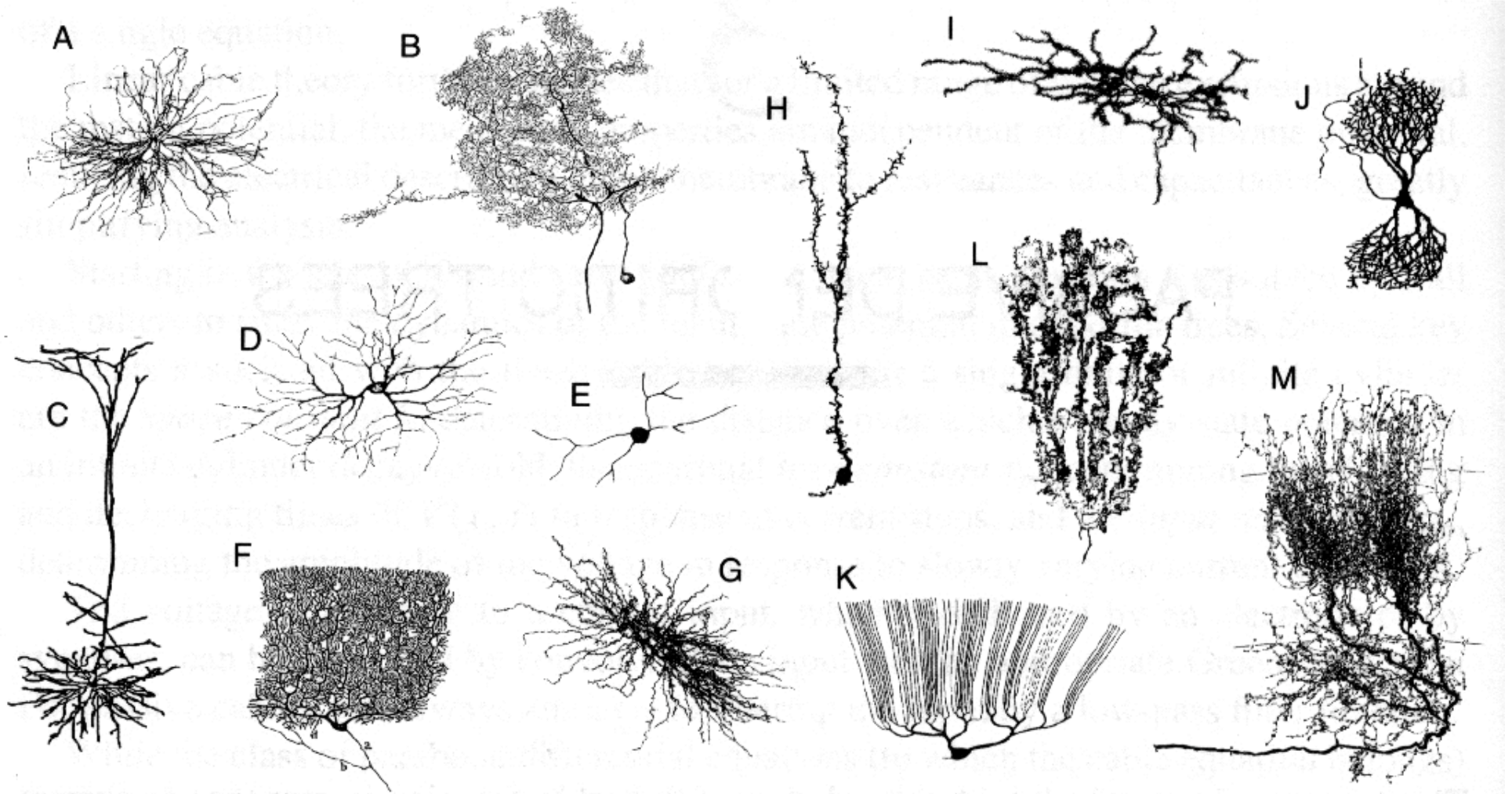
Temporal and Spatial Summation

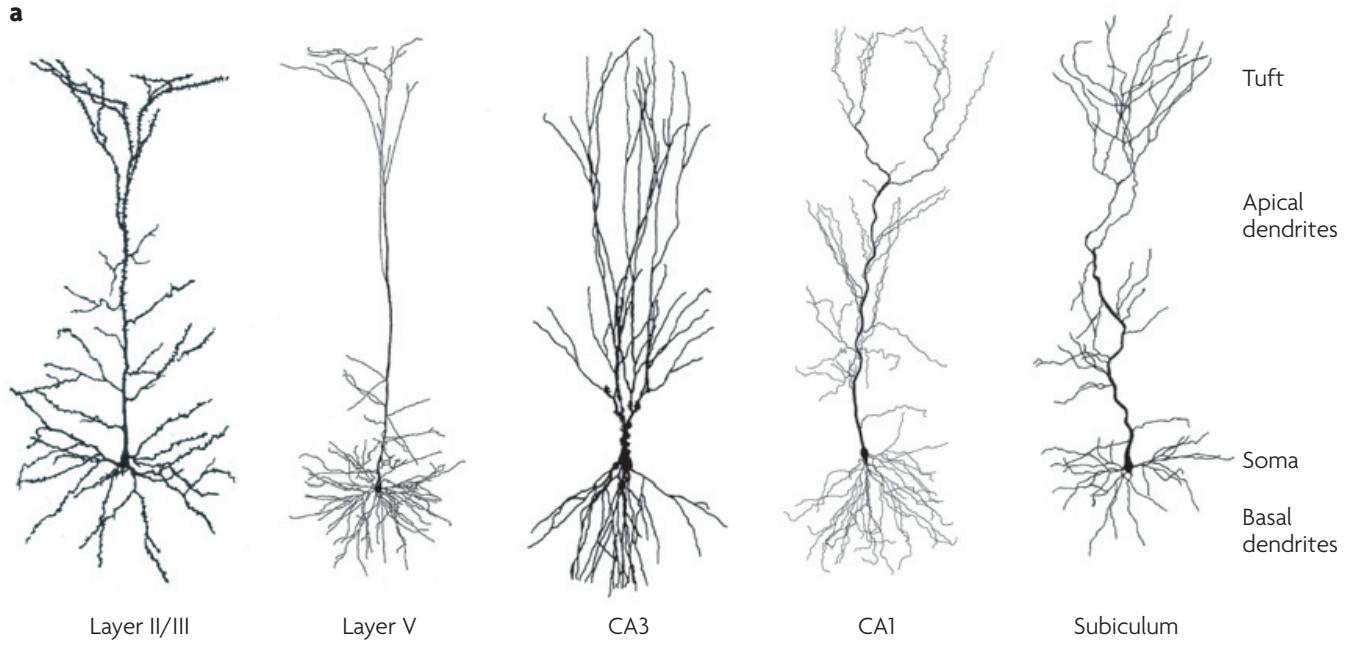






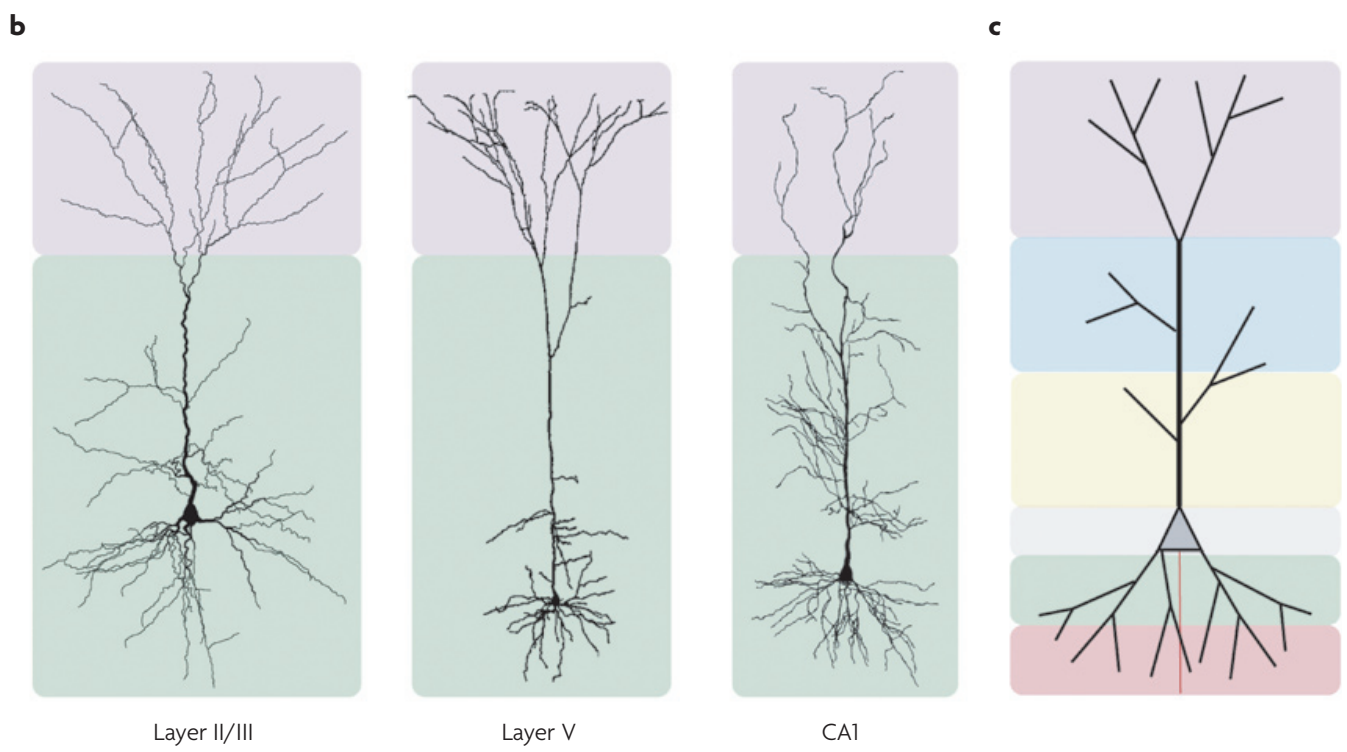
Spheres and Cables



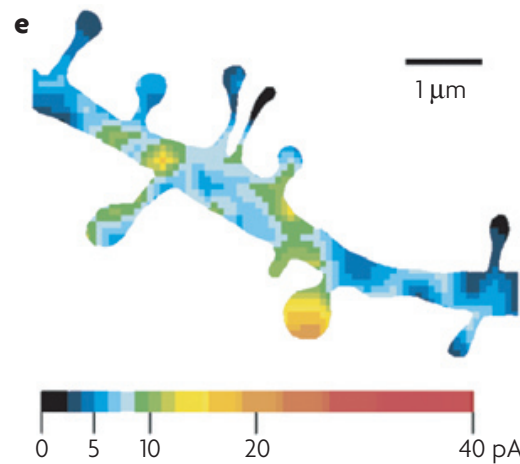
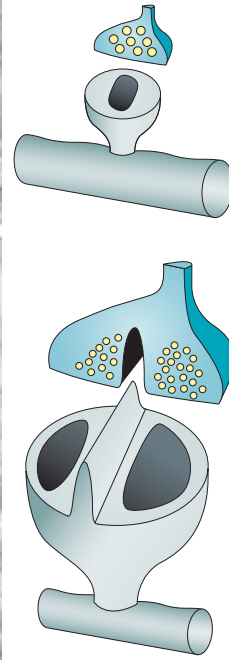
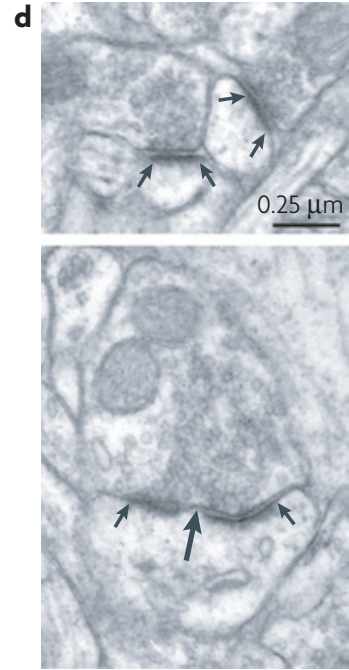
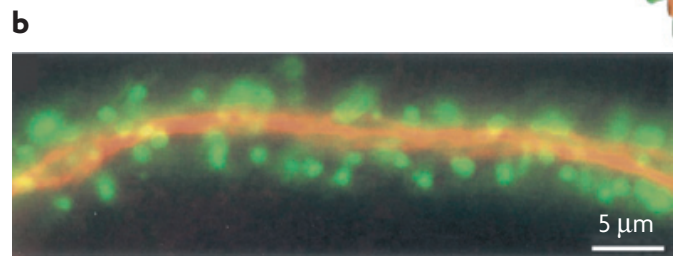


Pyramidal Cell Terminology

- Apical
- Basal
- Oblique
- Primary
- Secondary
- Tuft
- Branch point



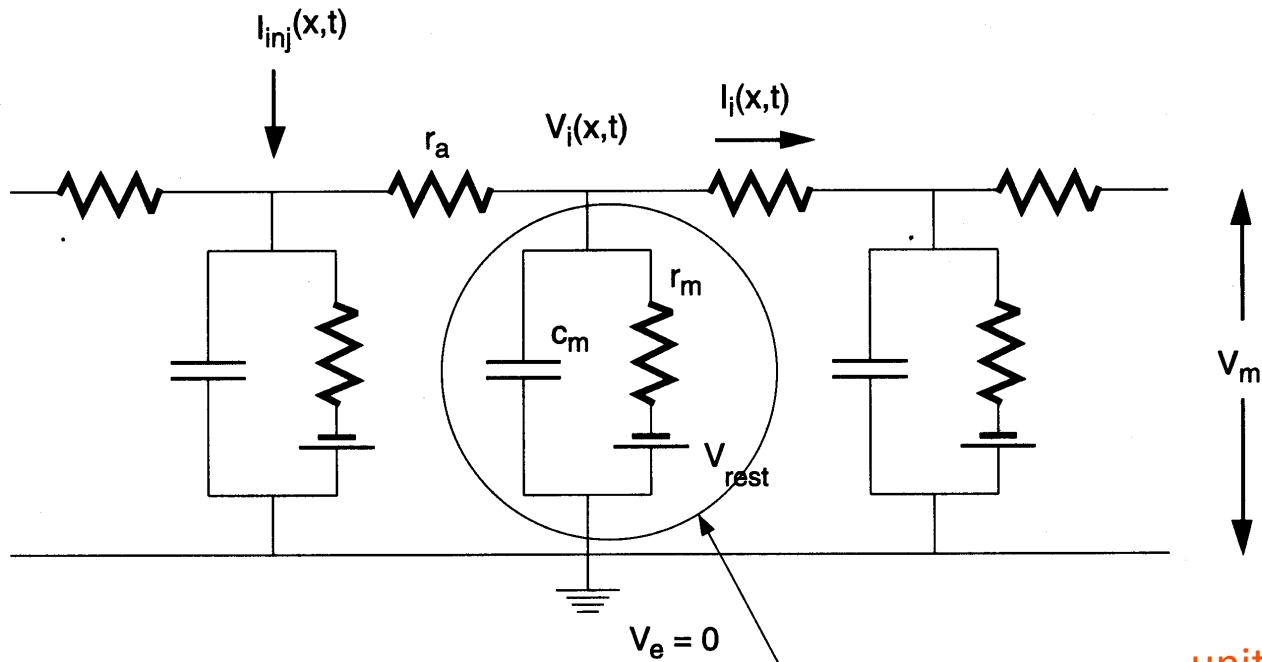
N. Spruston
 Nature Reviews
 Neurosci. (2008)



Spruston
(2008)

Modeling Dendritic Dynamics

– Rall Model



r_m : ohm-cm

r_a : ohm/cm

i_m : A/cm

c_m : F/cm

units:

$$\frac{1}{r_a} \frac{\partial^2 V_m(x,t)}{\partial x^2} = i_m(x,t)$$

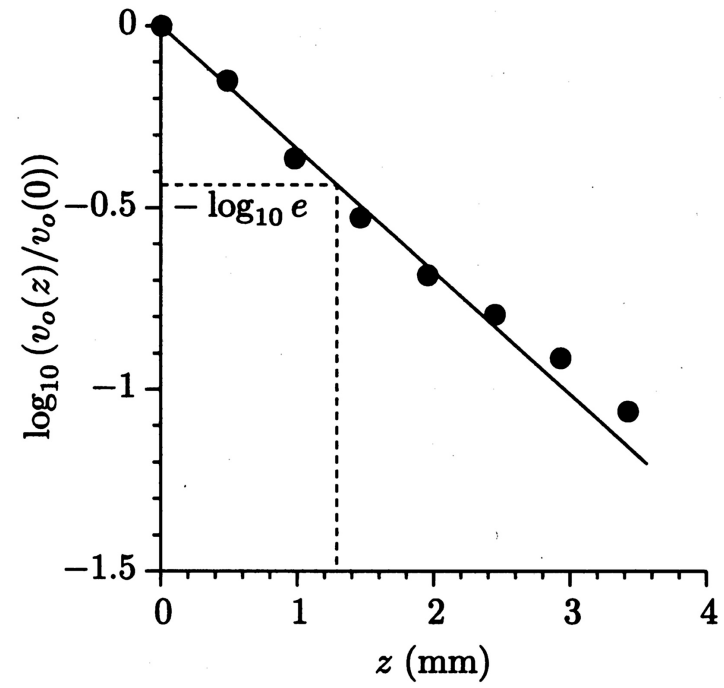
$$i_m(x,t) = \frac{V_m(x,t) - V_{rest}}{r_m} + c_m \frac{\partial V_m}{\partial t} - I_{inj}(x,t)$$

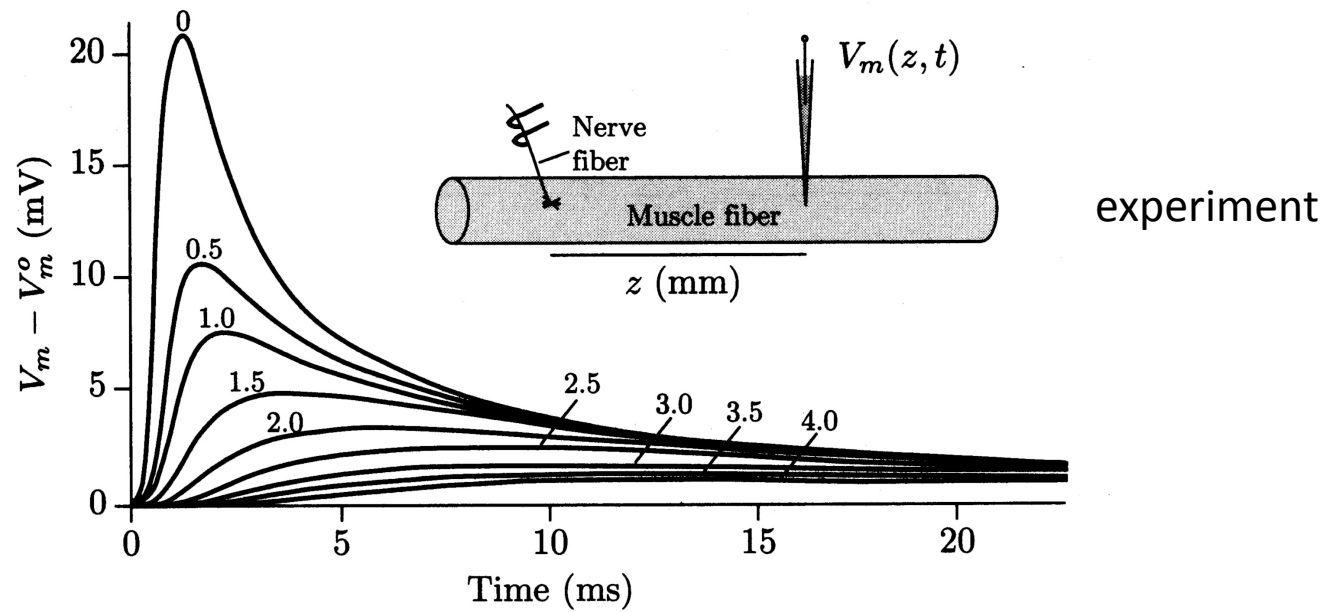
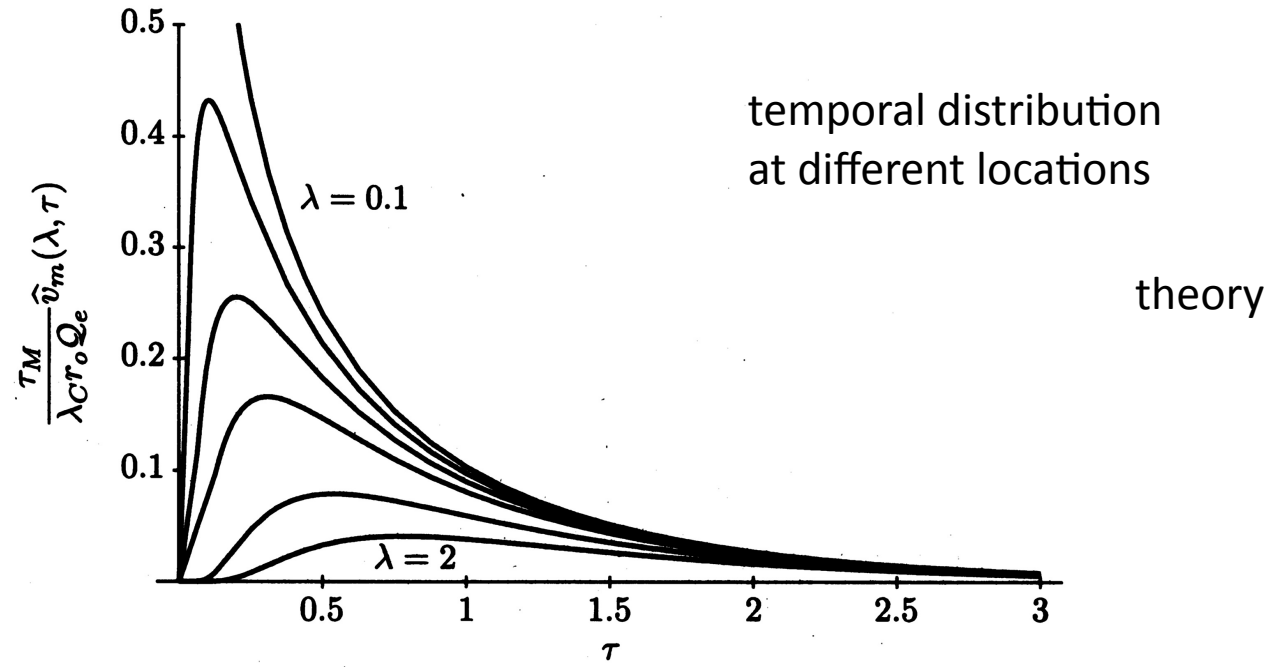
$$\lambda^2 \frac{\partial^2 V_m(x,t)}{\partial x^2} = \tau_m \frac{\partial V_m(x,t)}{\partial t} + (V_m(x,t) - V_{rest}) - r_m I_{inj}(x,t)$$

$$\tau_m = r_m c_m$$

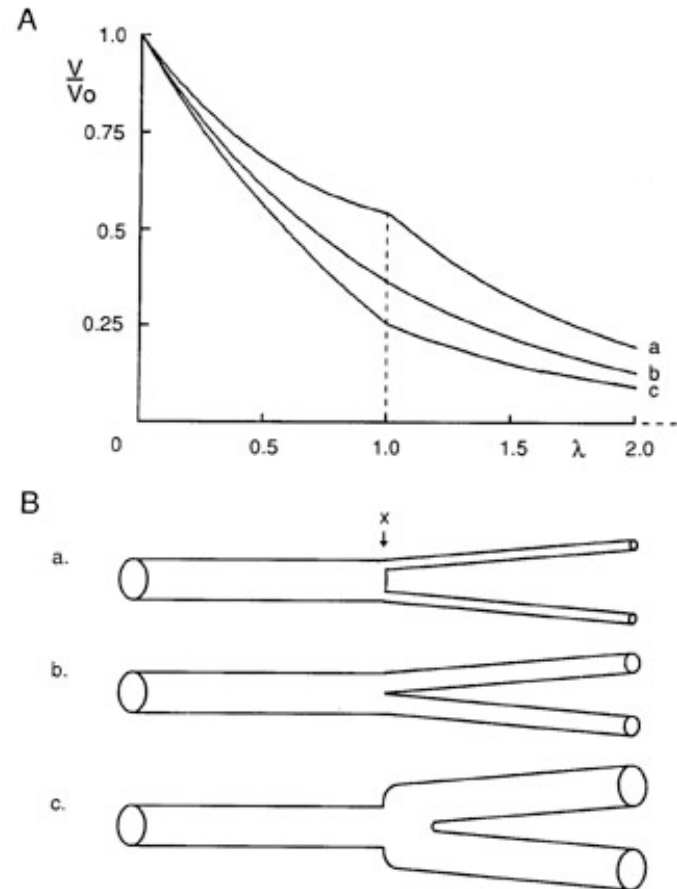
$$\lambda = \sqrt{\frac{r_m}{r_a}}$$

$$V(x) = V_0 \exp(-|x|/\lambda)$$





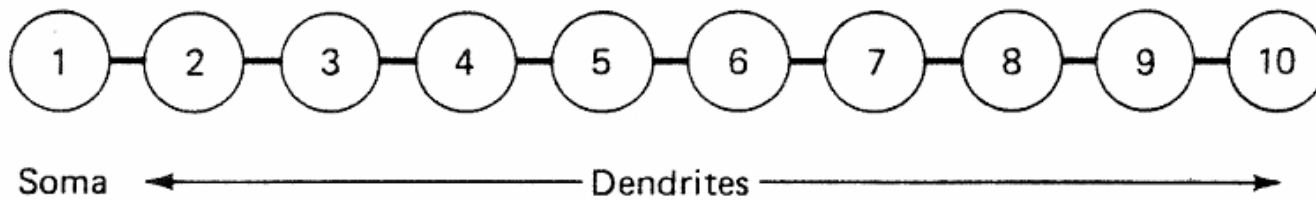
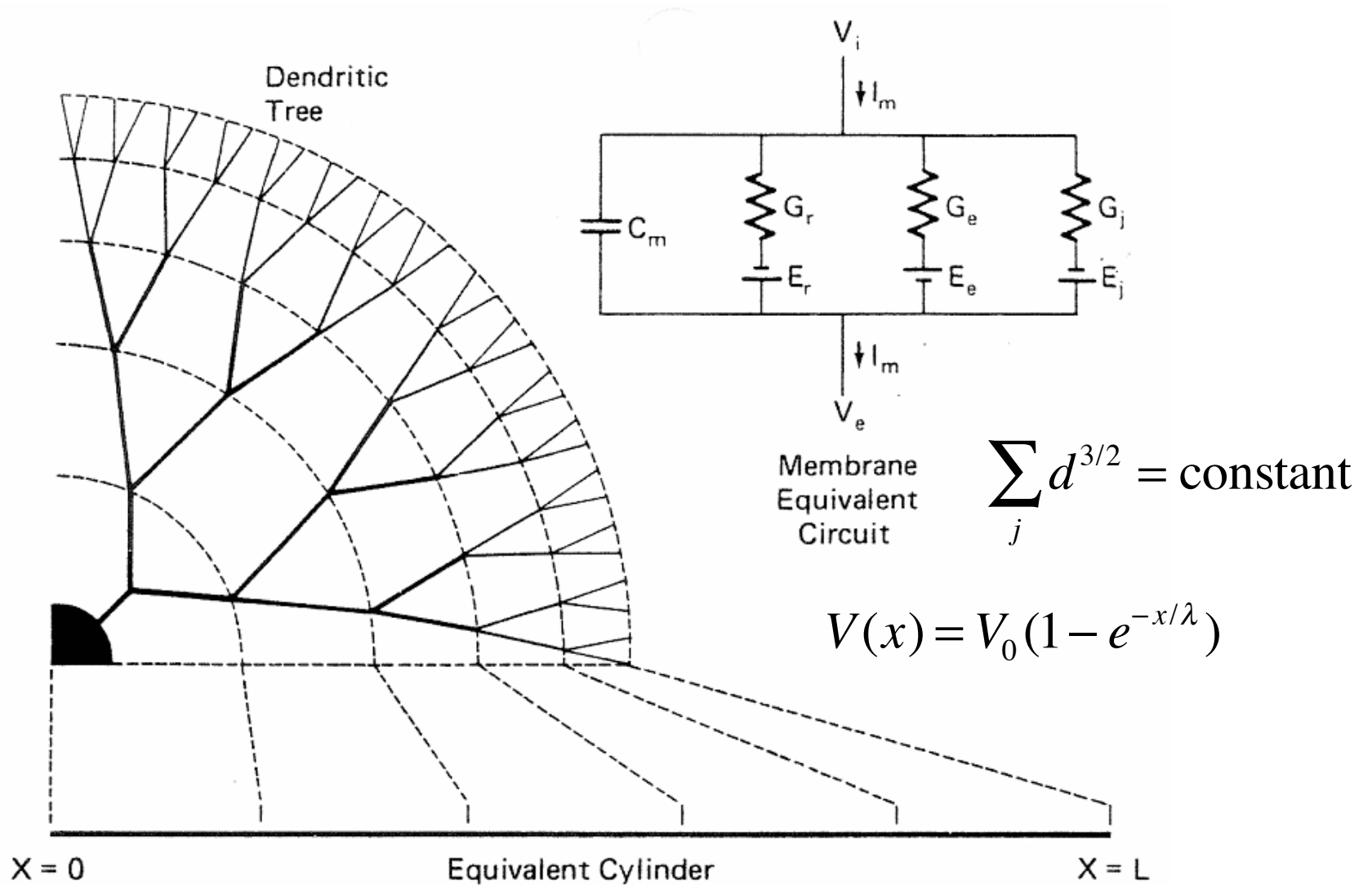
Voltage attenuation in branching cables

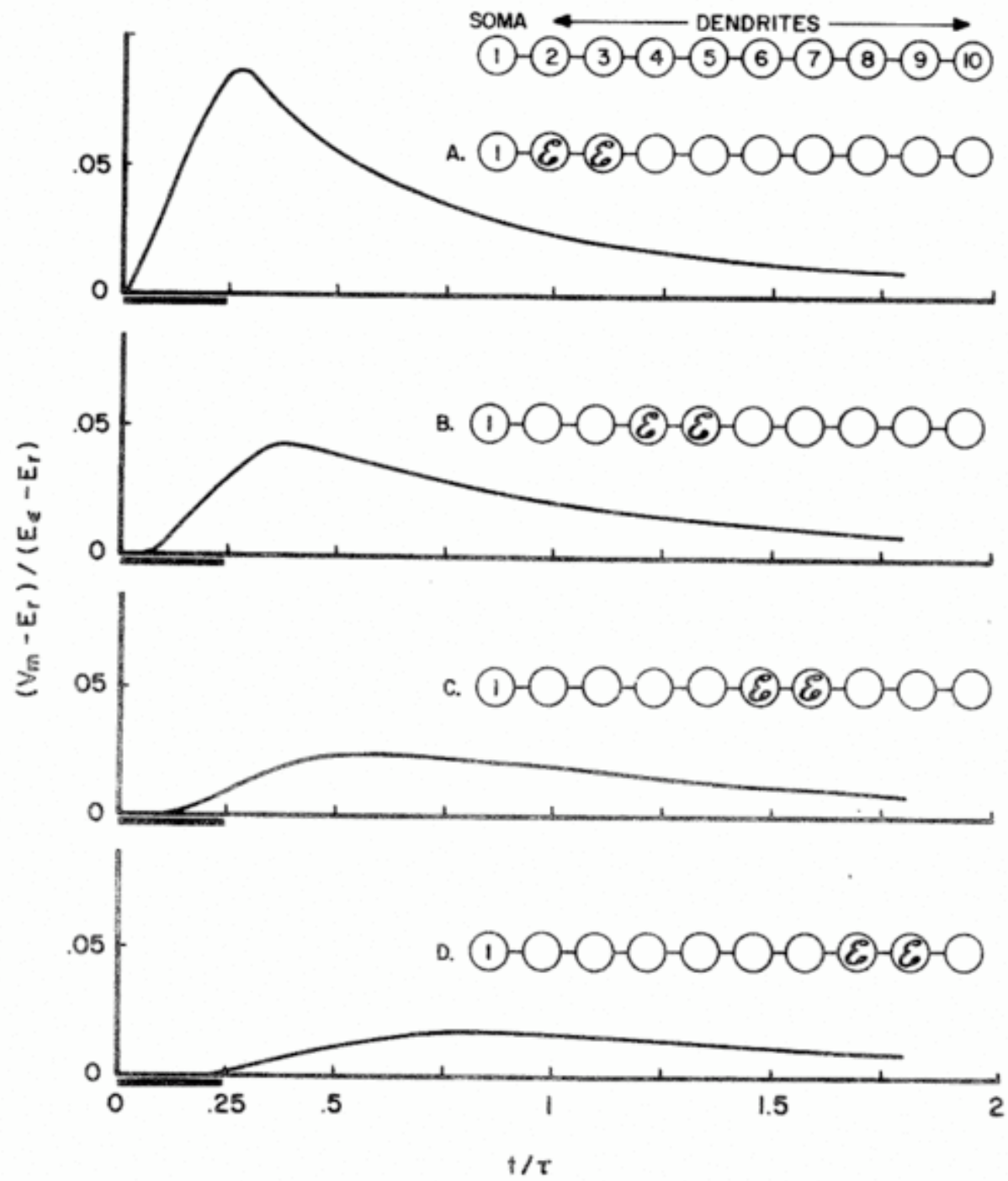


$$d_1^{3/2} = d_{21}^{3/2} + d_{22}^{3/2}$$

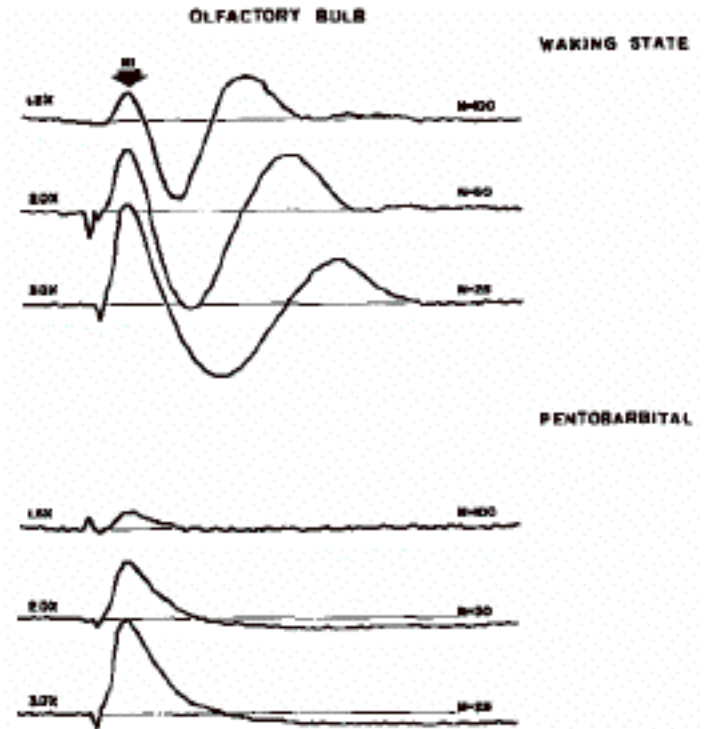
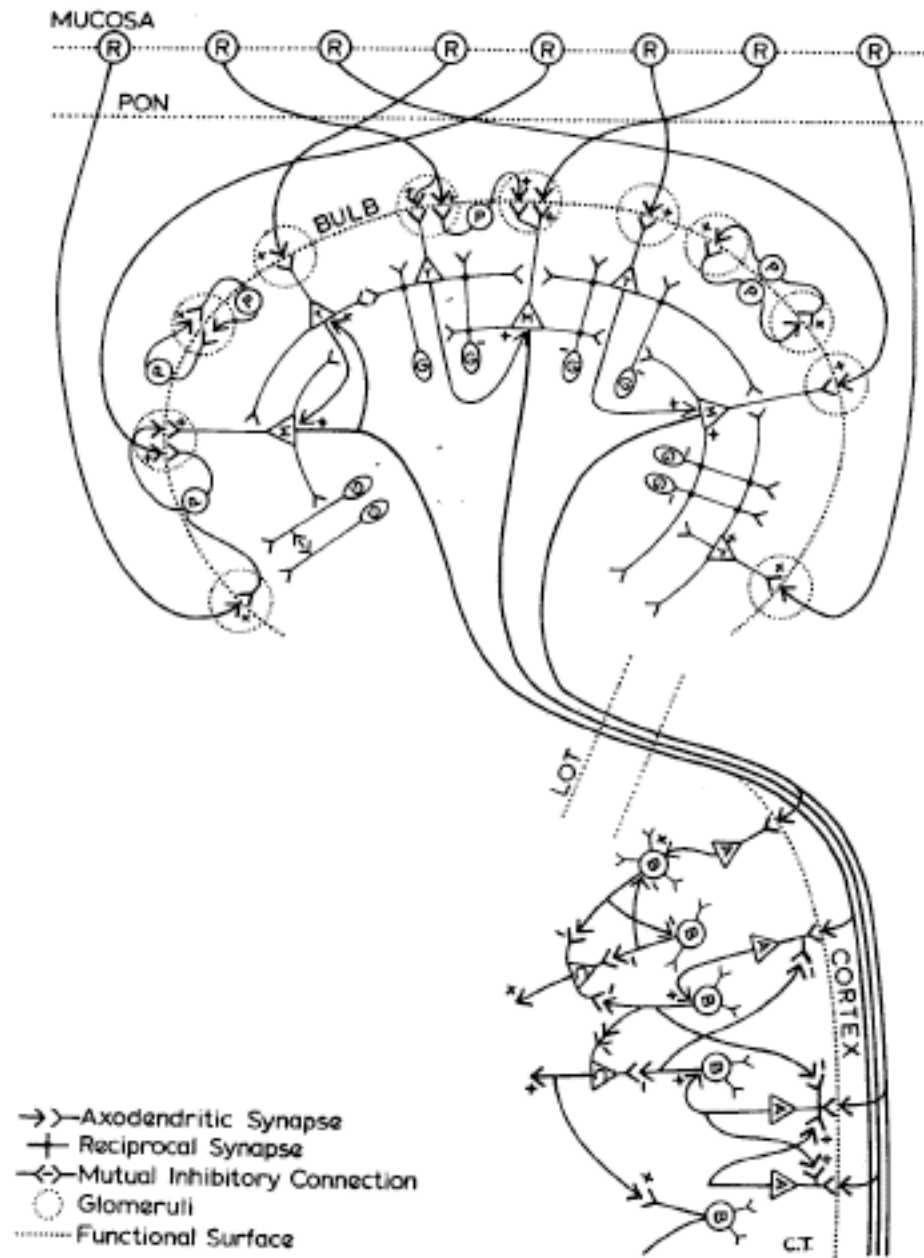
FIG. 13.7. Effect of different modes of dendritic branching on the spread of electrotonic potential. **A.** Graph of steady-state potential spread for the three cases illustrated in **B.** **B.** Diagrams illustrating three basic modes of branching; in each case the stem diameter is $4 \mu\text{m}$: (a) Each daughter branch is $1 \mu\text{m}$ in diameter; (b) each daughter branch is approximately $2.5 \mu\text{m}$, so that sum of $d^{3/2}$ equals $d^{3/2}$ of the stem; (c) each daughter branch has the same diameter as the stem. (Modified from Rall, 1958.)

Modeling Spinal Motor Neurons

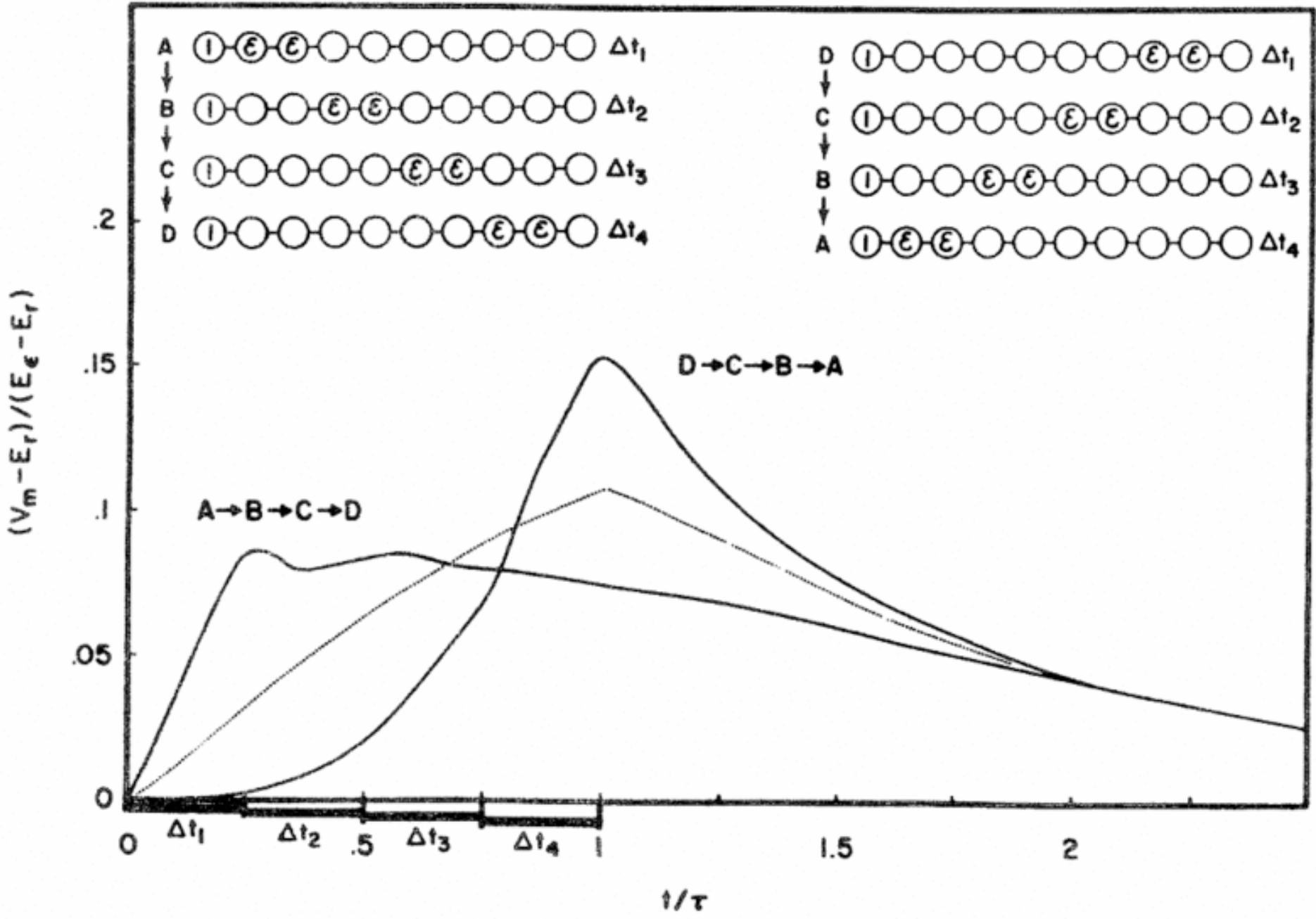




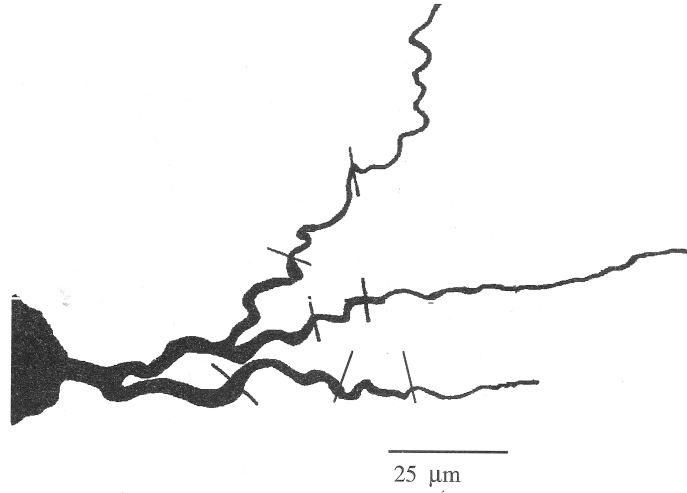
Rall & Shepherd – Evoked potential in OB



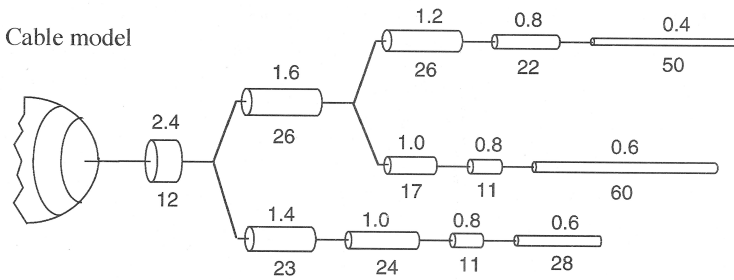
Sequencing Effects of Time Delay for Distal Synapses



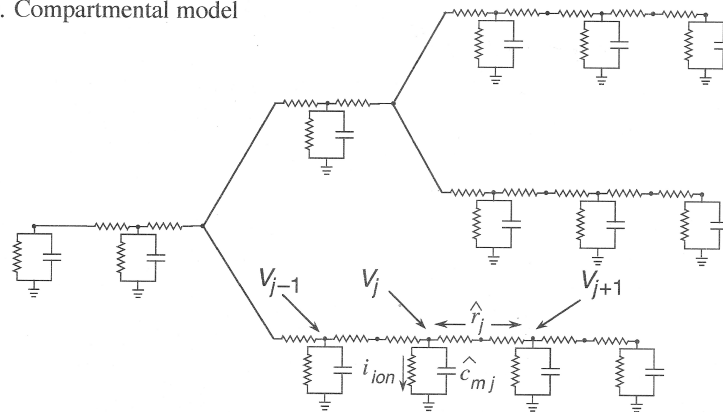
a. Physiologically and morphologically characterized neuron



b. Cable model




c. Compartmental model



Documentation | NEURON

http://www.neuron.yale.edu/neuron/docs

Blackboard ...demic Suite ExpressPCB ...nufacturing Diamond Turnability Google Imag...eBuckle.jpg Apple



NEURON

for empirically-based simulations of neurons and networks of neurons

[NEURON news](#) | [Download](#) | [Courses](#) | [About](#)
[Documentation](#) | [Programmer's Reference](#) | [Forum](#) | [Resources](#) | [ModelDB](#)

Documentation

[FAQ](#)
[Programmer's Reference](#)
Get a pkzip archive of the Programmer's Reference
The mercurial repository change log and sources

Tutorials

[Construction and Use of Models: Part 1. Elementary Tools](#)
A good place to start. Introduces some of NEURON's basic GUI tools.

[Import3D tutorial](#)
A convenient GUI tool for converting Eutectic, NeuroLucida, and swc morphometric data into NEURON models. This used to be [../docs/import3d/main.html](#)

[CellBuilder tutorial](#)

Search

Search this site:

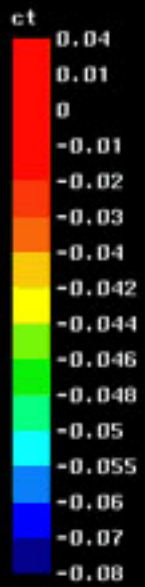
Navigation

- ▶ [Blogs](#)
- [Recent posts](#)

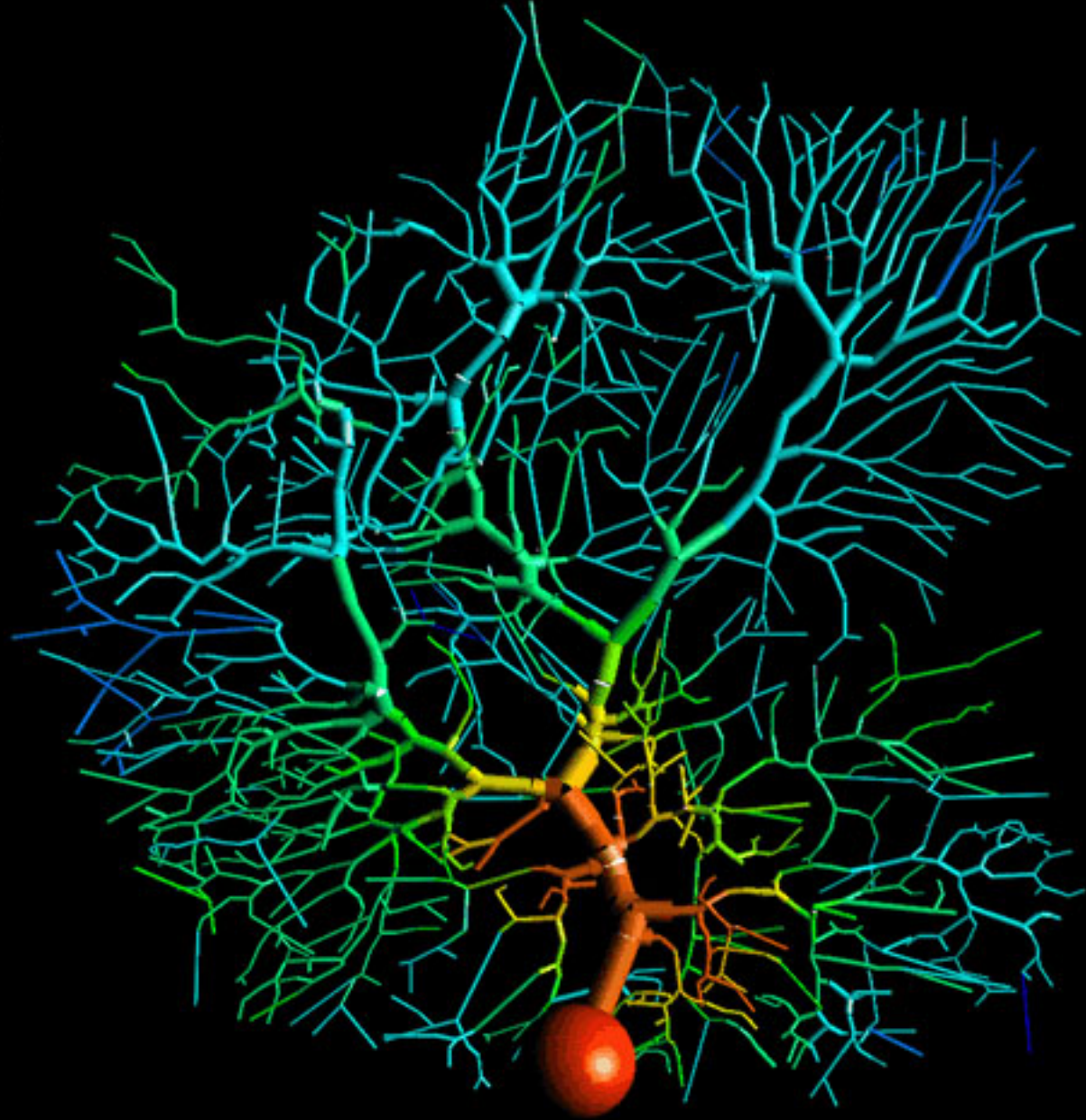
Recent blog posts

- [A new look and new functionality](#)
- [Previous news and milestones](#)

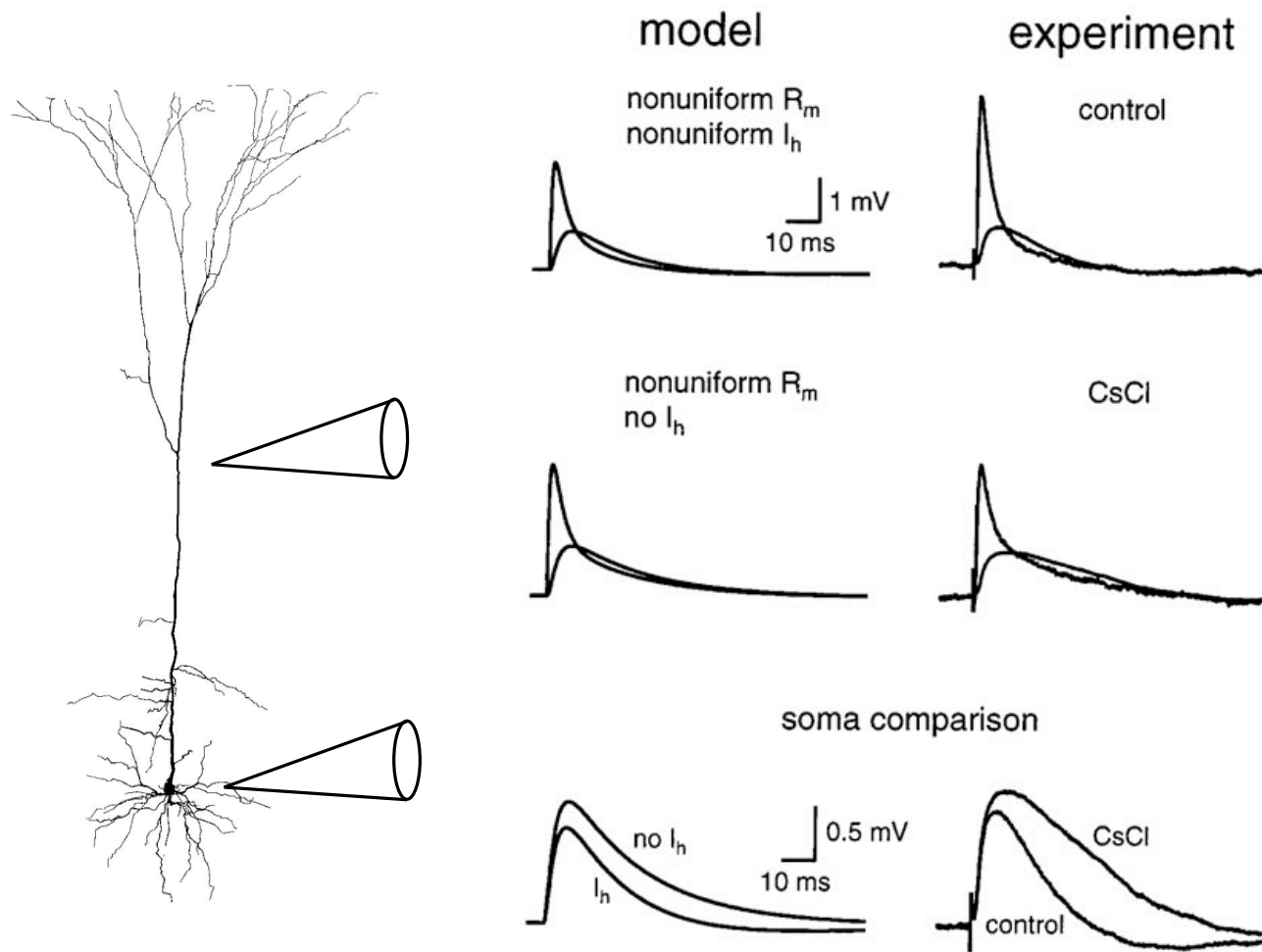
0.009700



0.0313455 μm

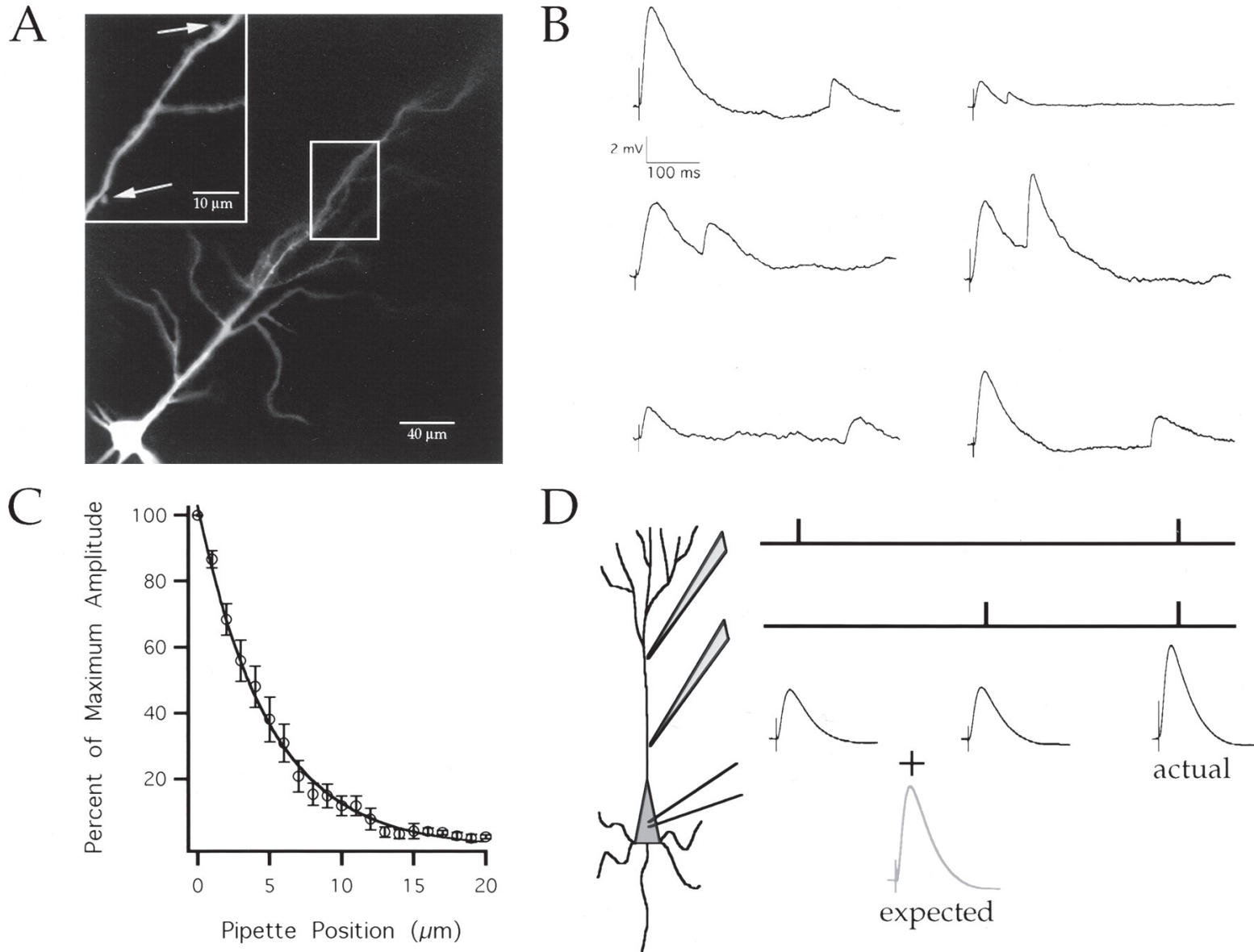


EPSP attenuation in dendrites of pyramidal neurons

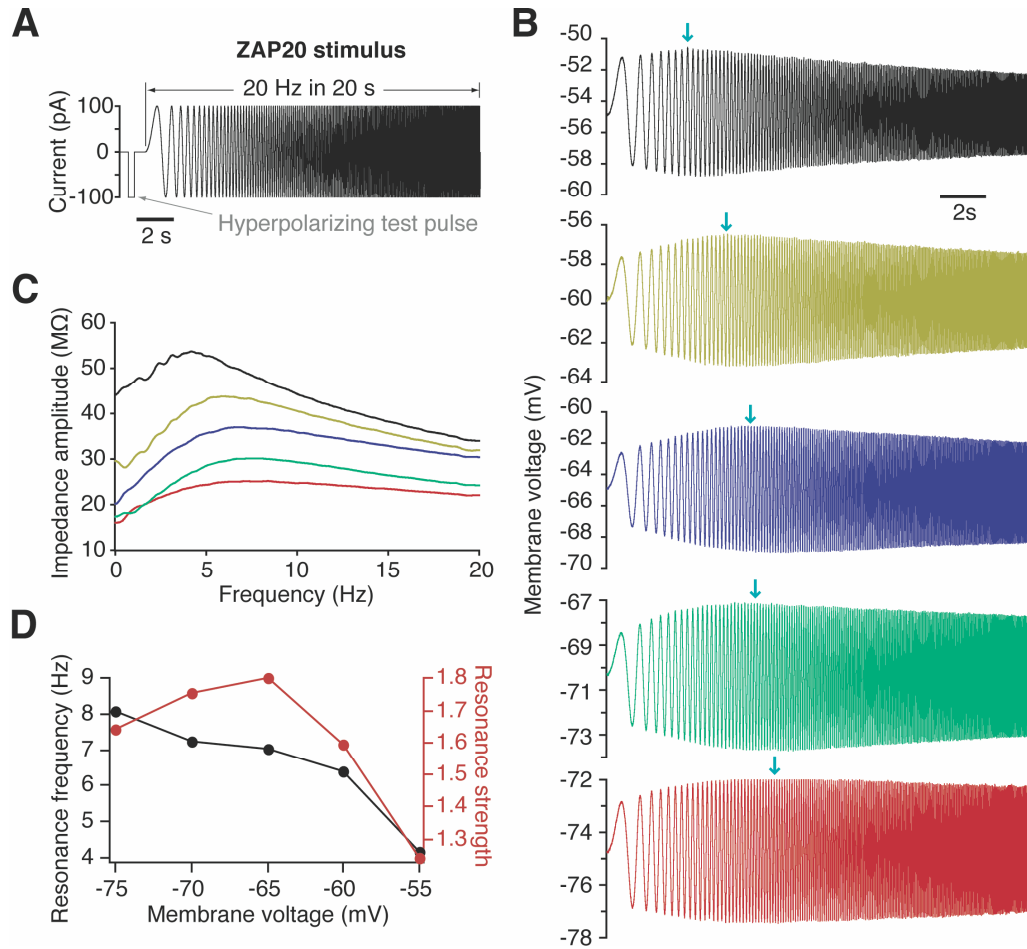


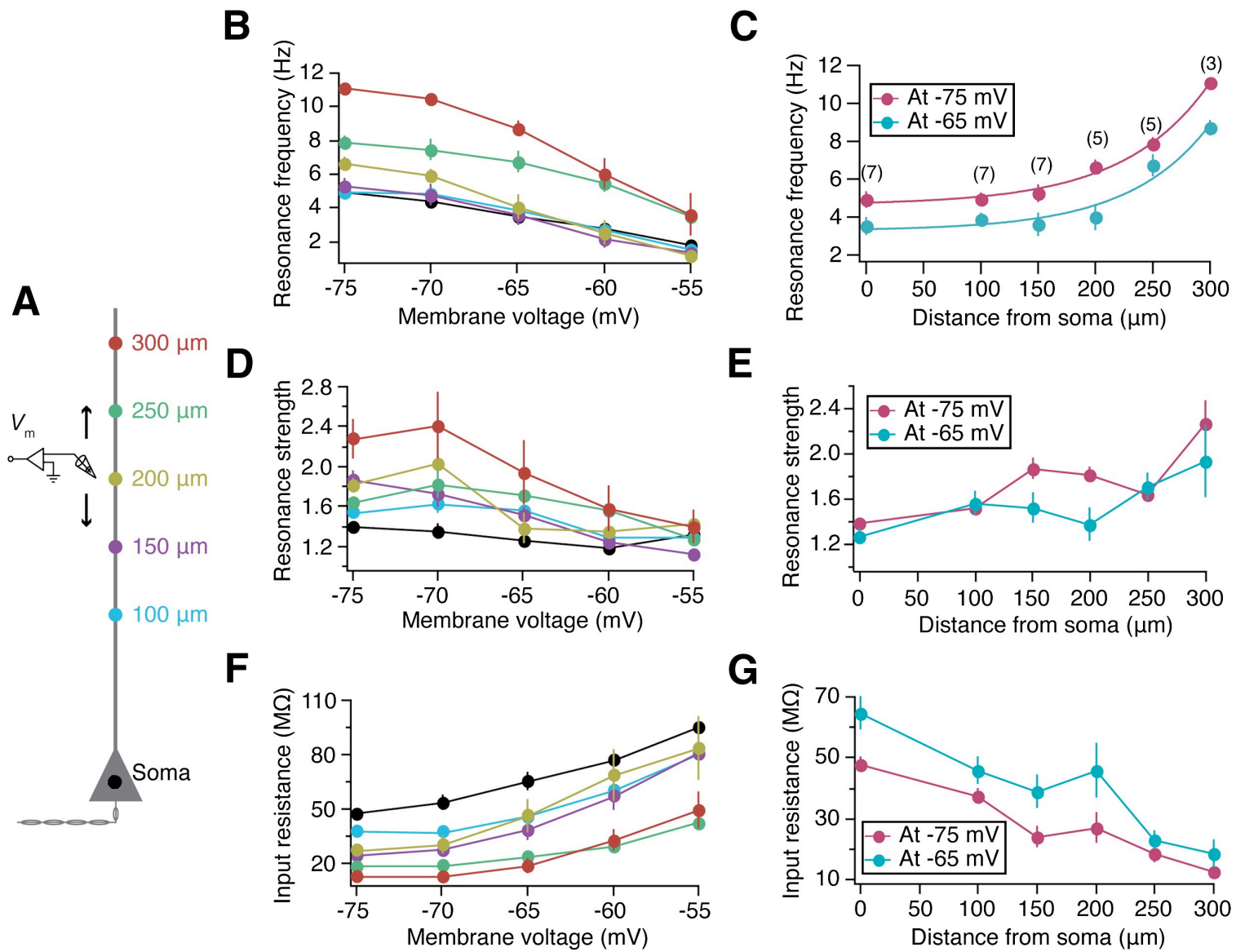
Stuart & Spruston, 1998

Spatial Summation in Dendrites: Evidence for Linearity



Voltage dependent channels (h current) Resonance Properties in Dendrites

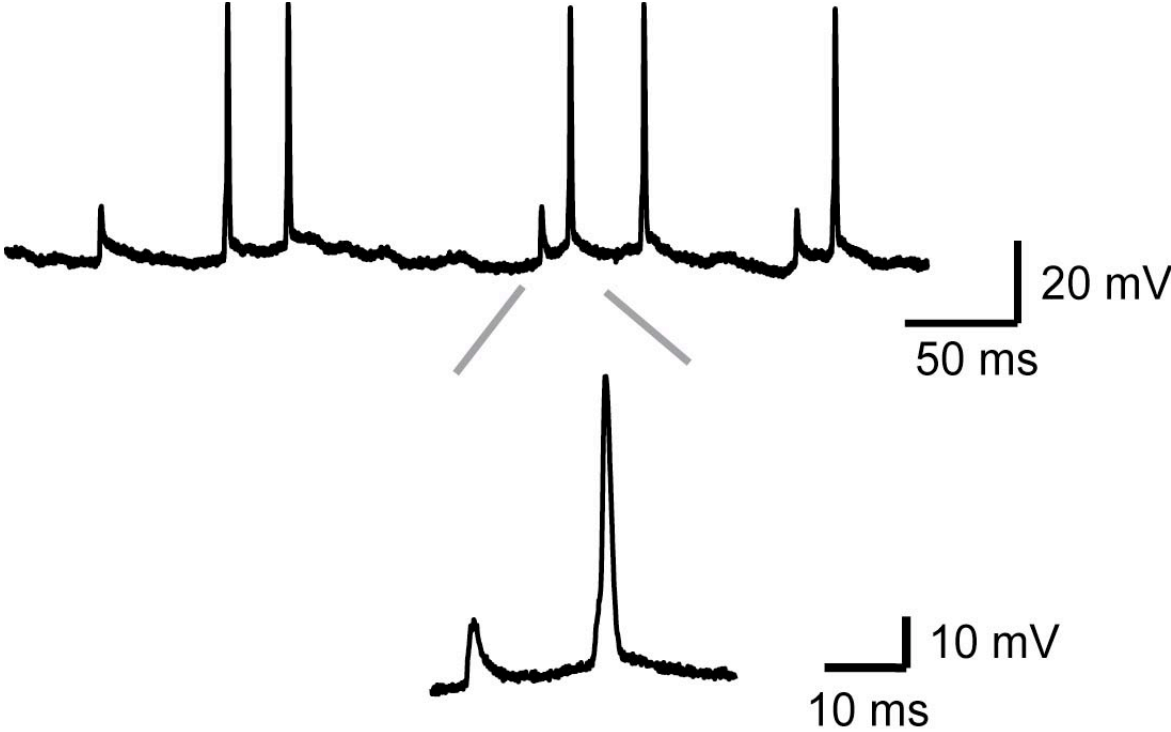


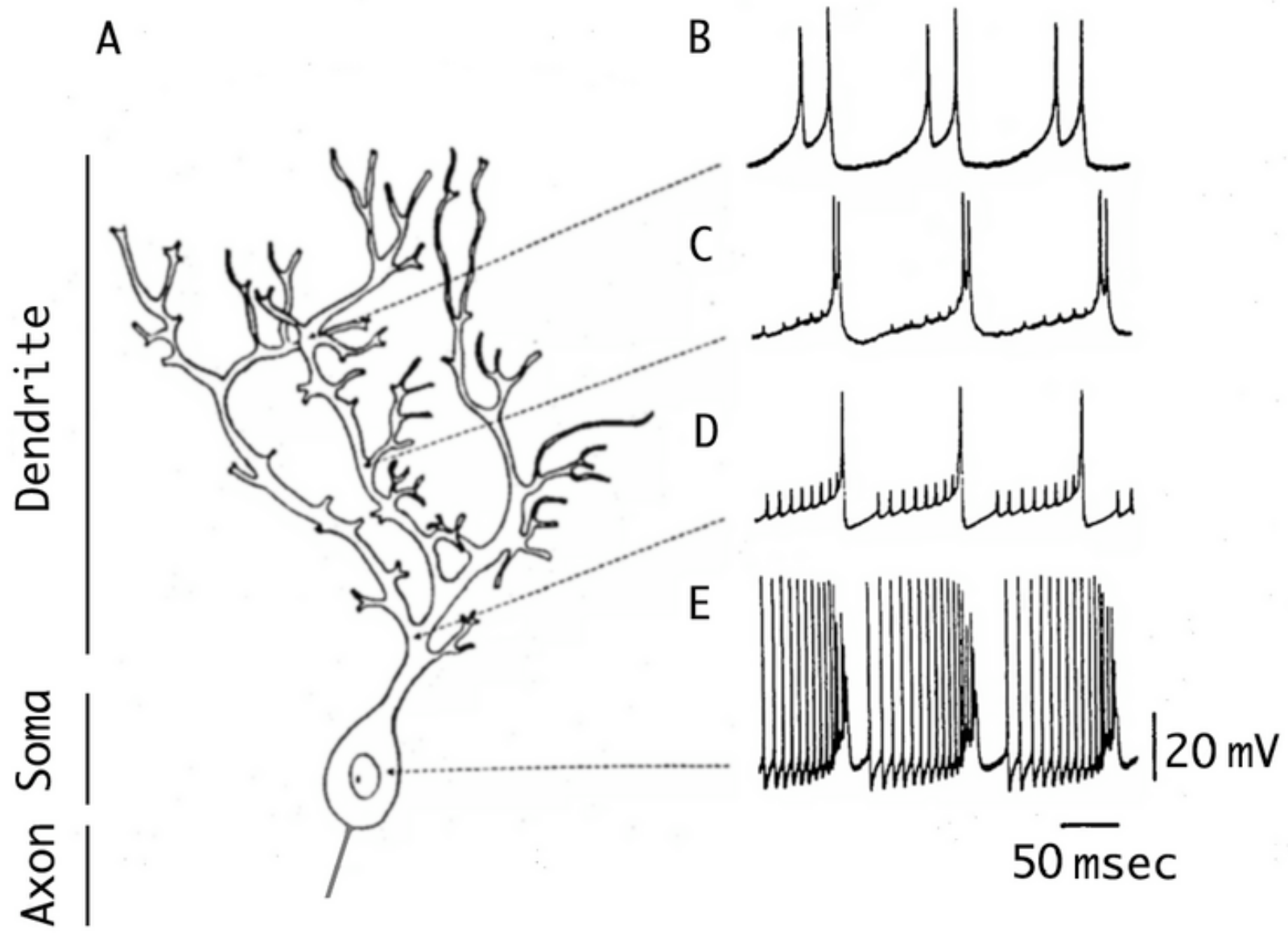


Active Dendrites

Spencer and Kandel

“prepotentials”





Llinas & Sugimori

New Techniques to Study Dendrites

Visualization (IR and Fluorescence)

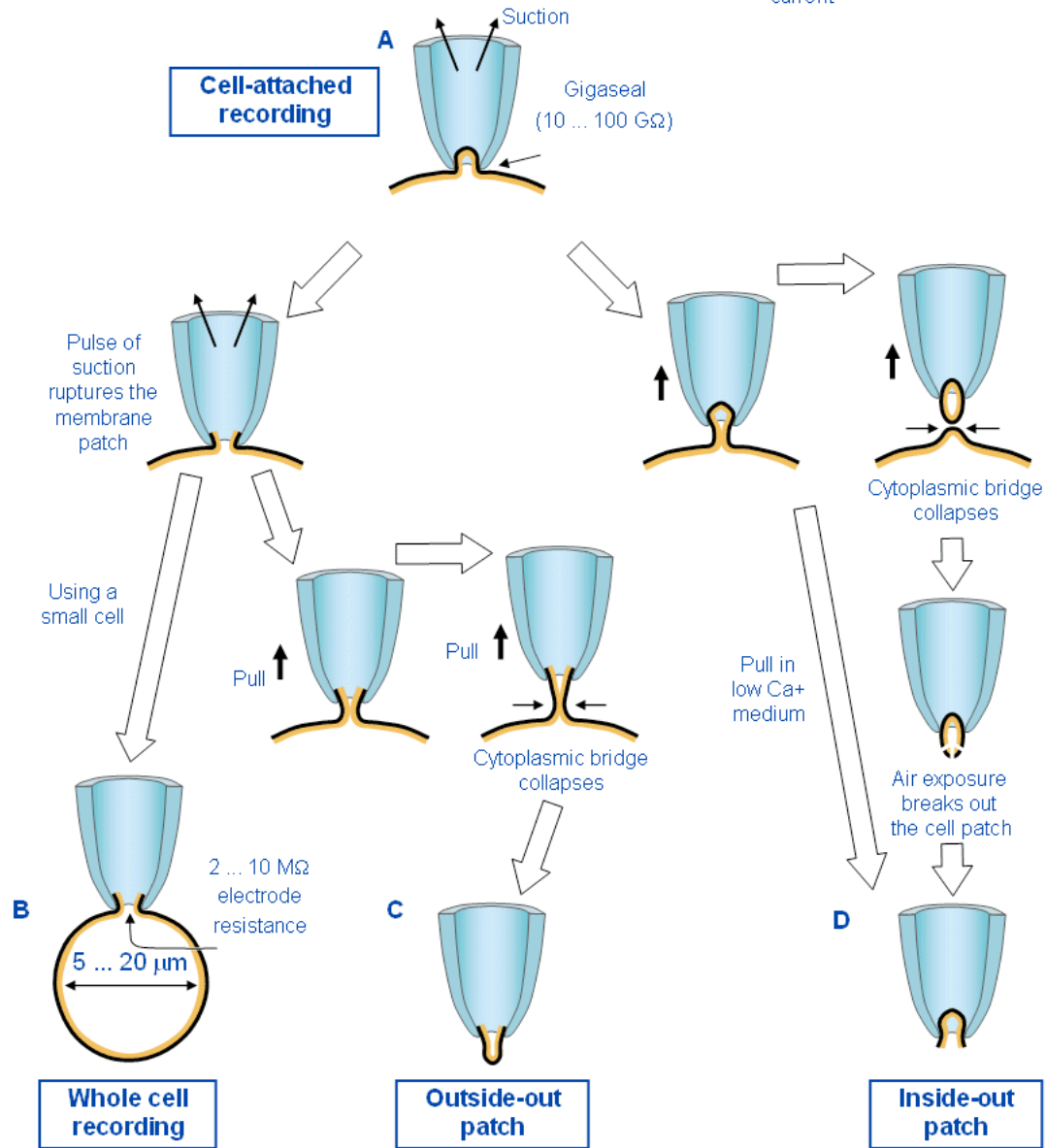
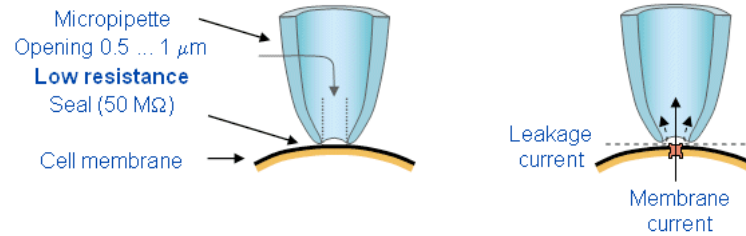
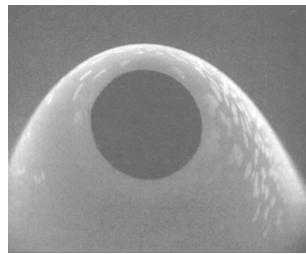
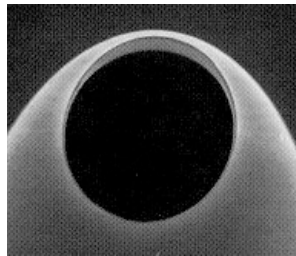
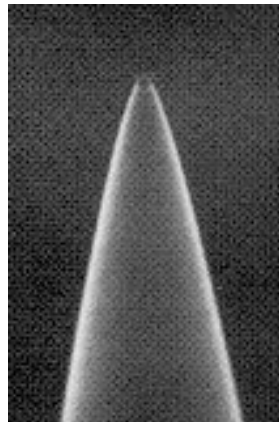
Patch recording from dendrites

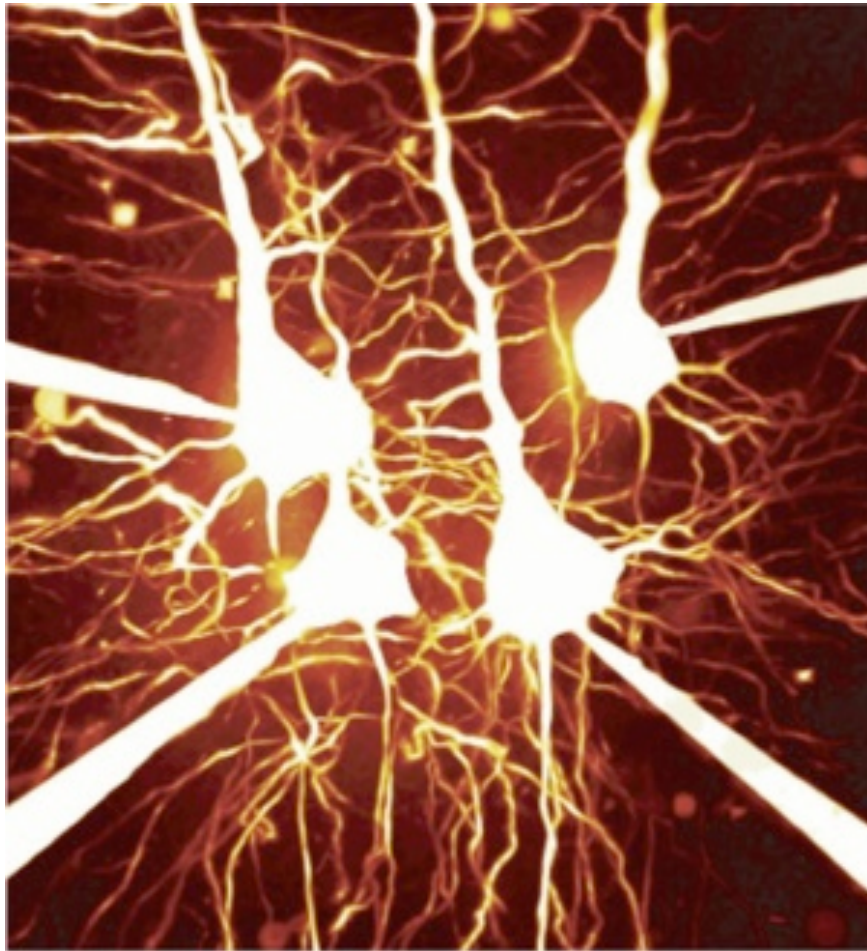
Two photon laser scanning microscopy

Calcium concentration dynamics

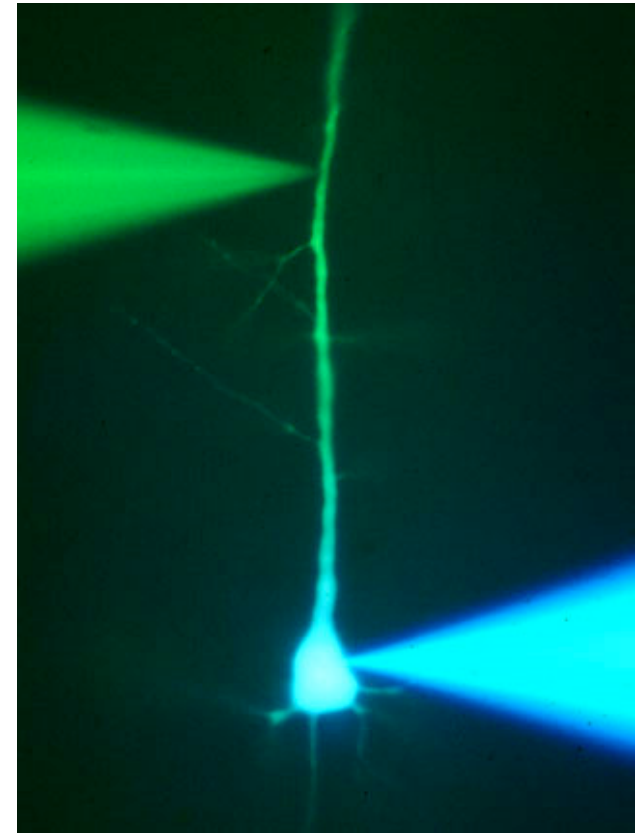
Caged transmitters and two photon uncaging

Patch Recording

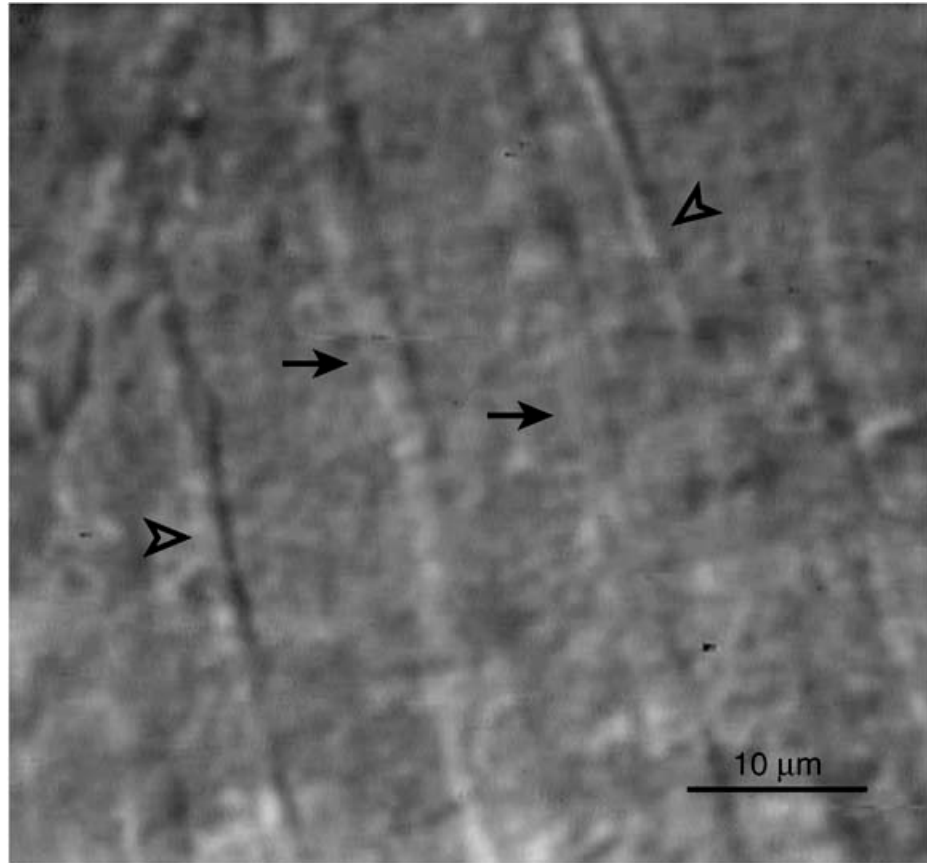




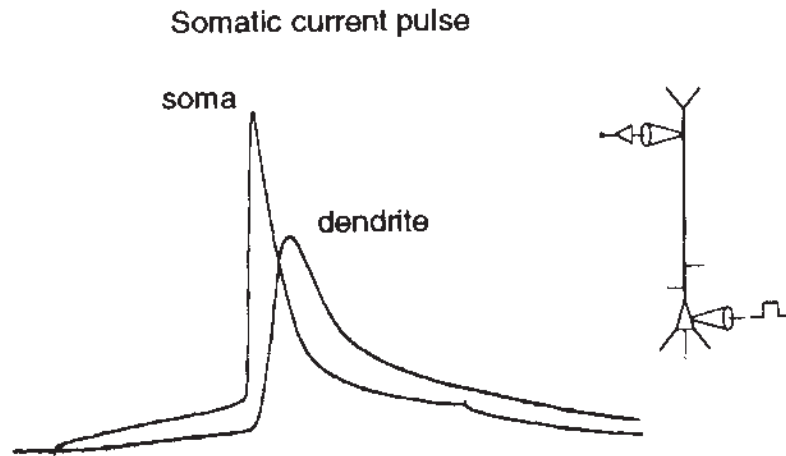
M. Hausser



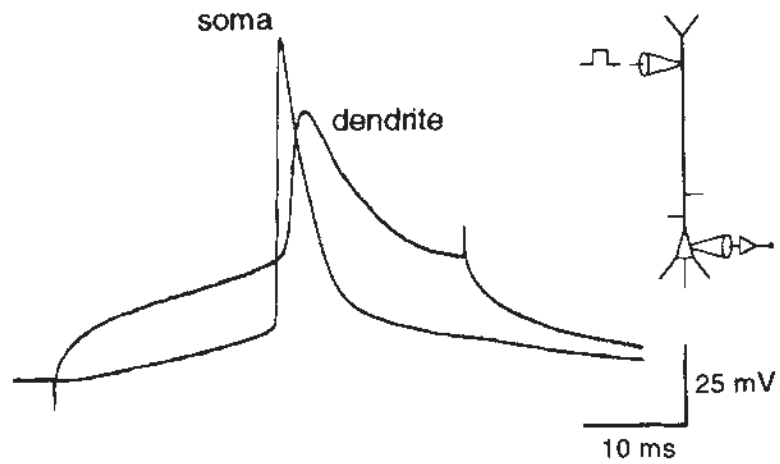
Diffusion, Visualization, and Dialysis



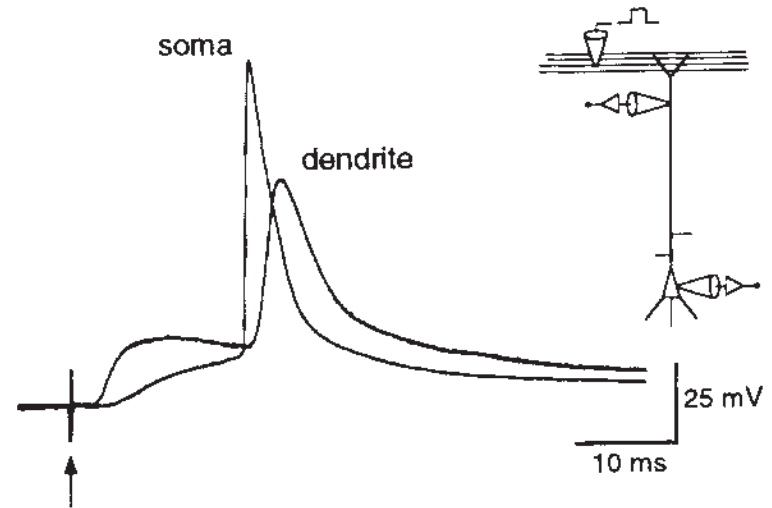
a



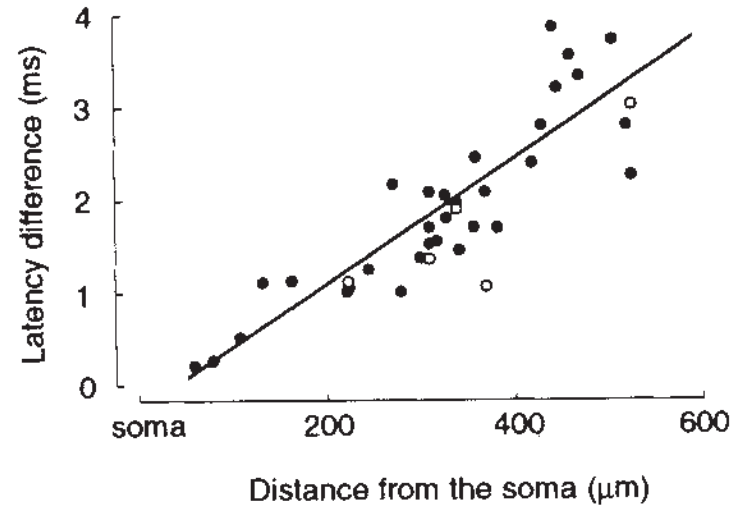
Dendritic current pulse



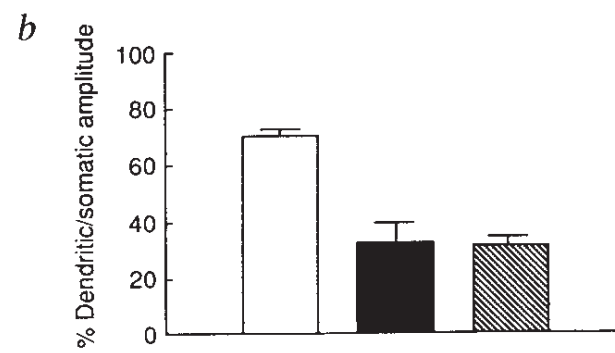
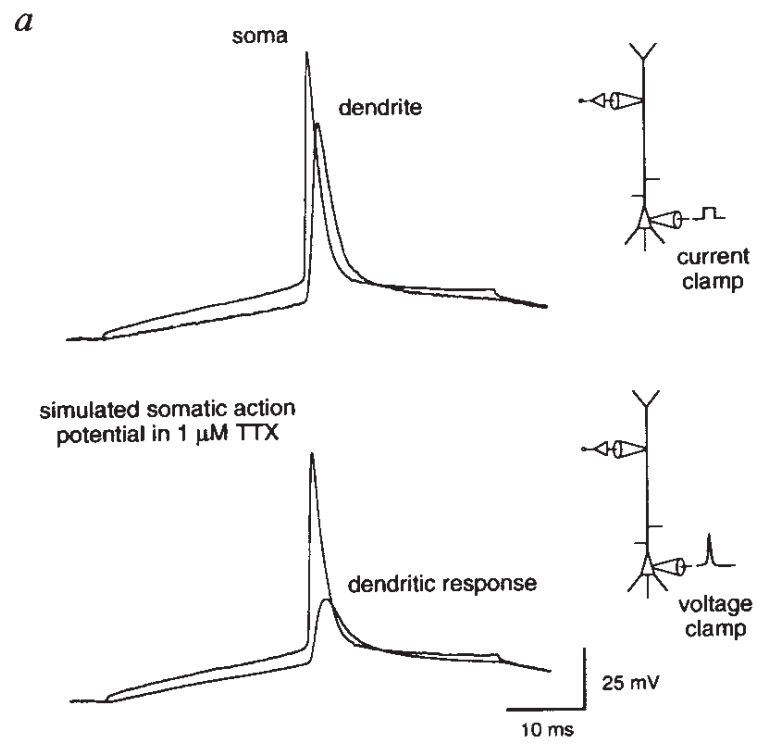
c



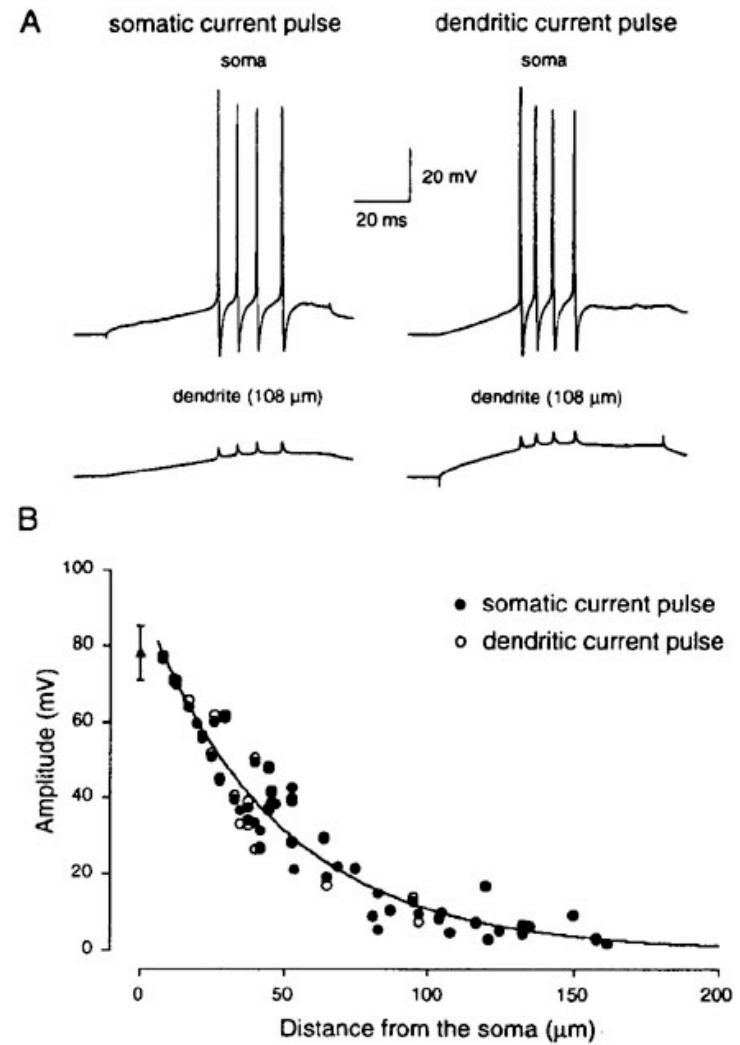
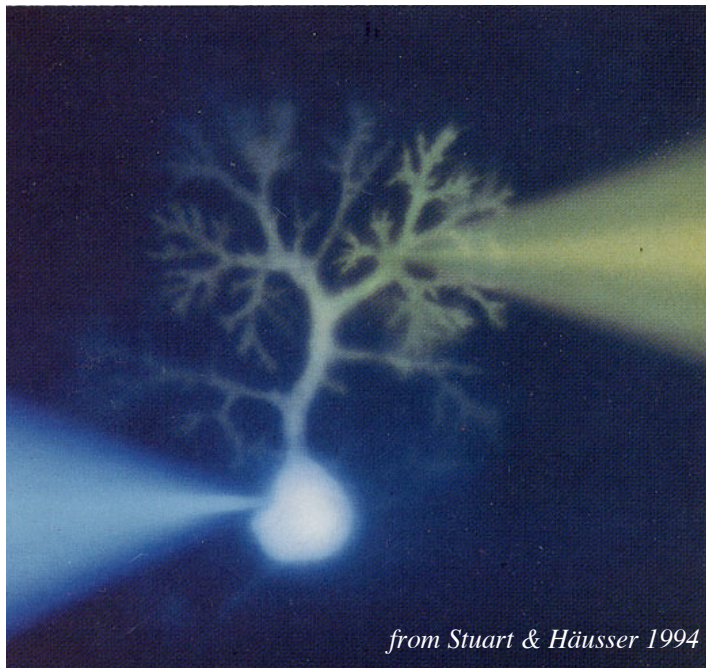
d



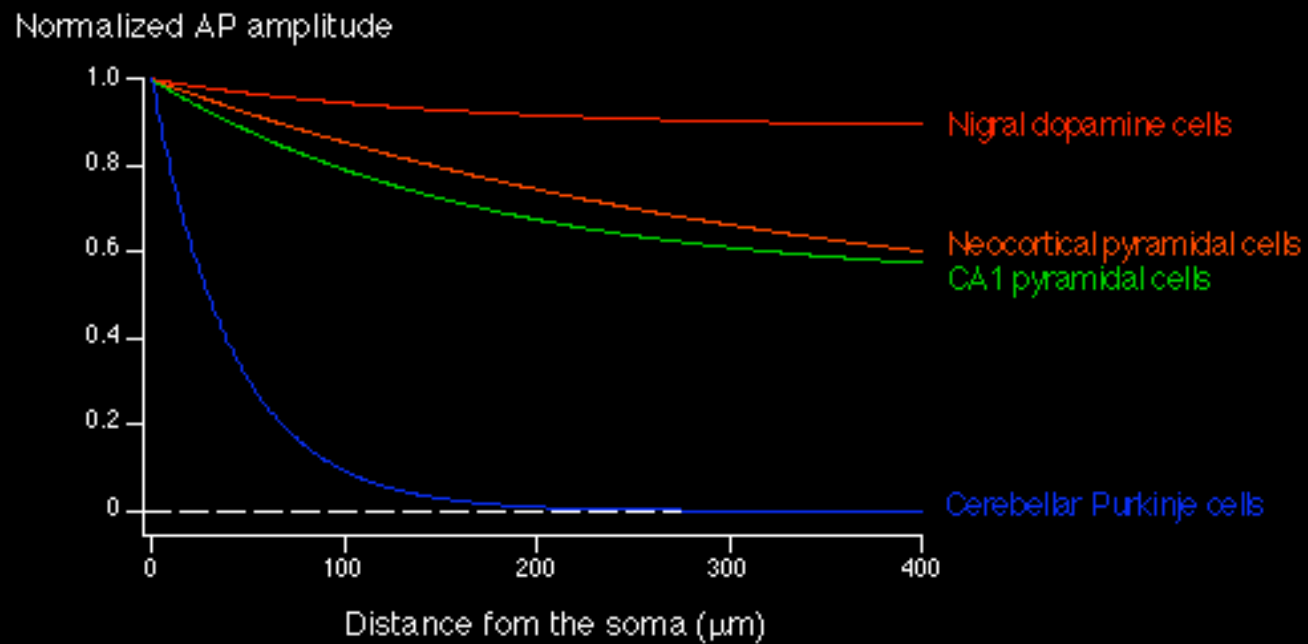
Stuart & Sakmann, Nature (1994)



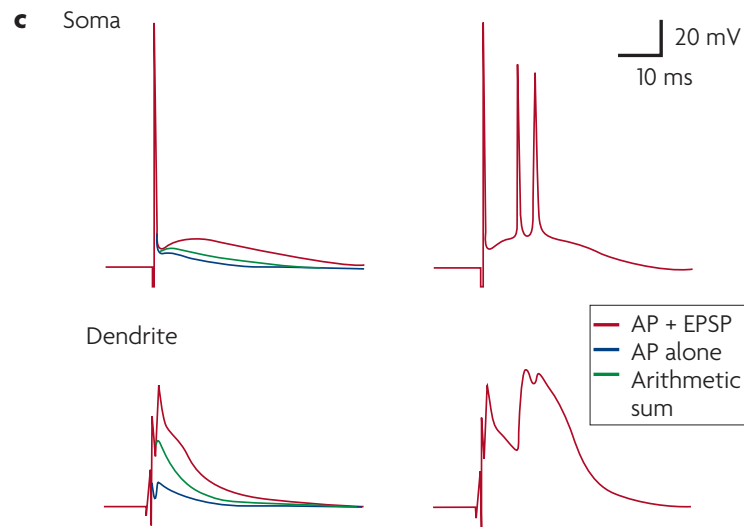
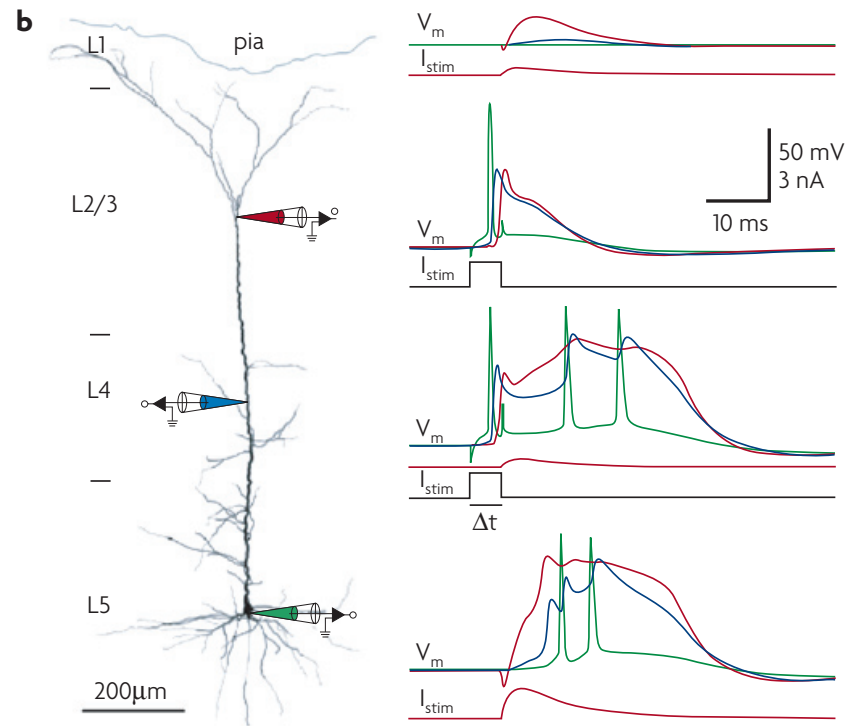
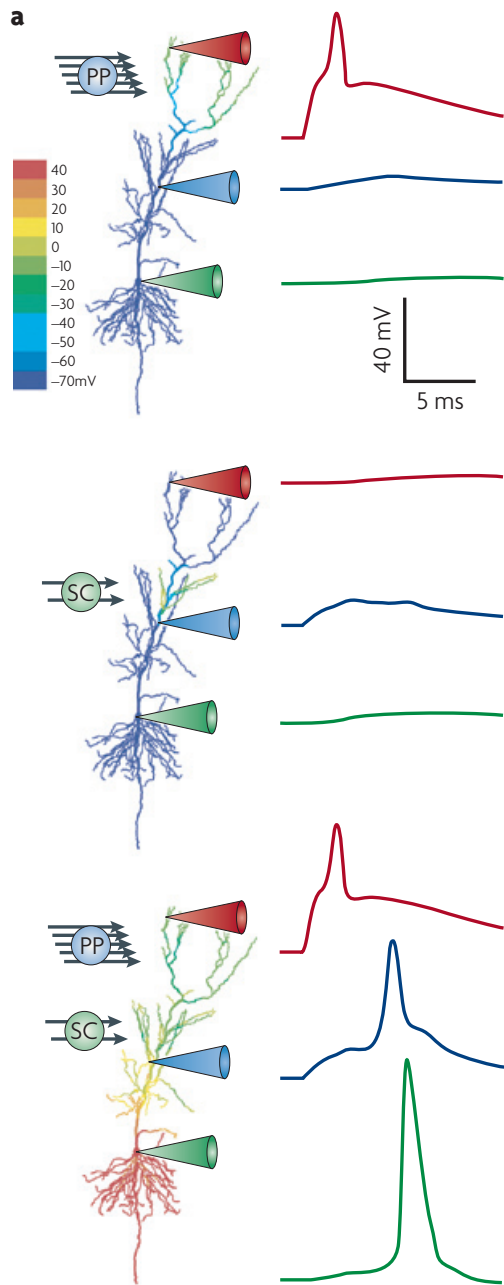
Backpropagation is not present in all neurons (e.g. Purkinje cells)



Backpropagation is cell-type specific



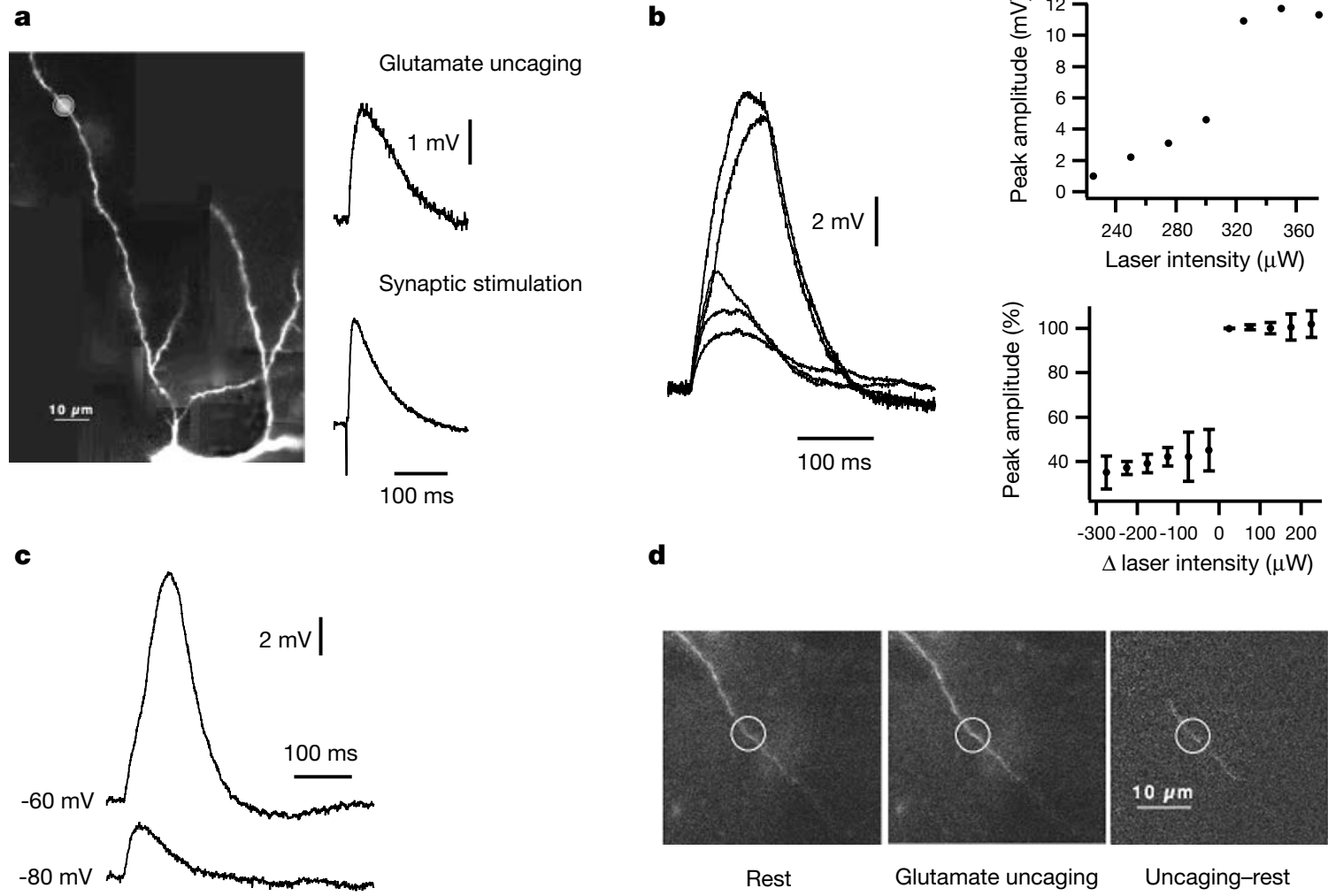
Nonlinear effects of mixed PSPs and Spikes



BAC: backprop.
activated calcium
spike

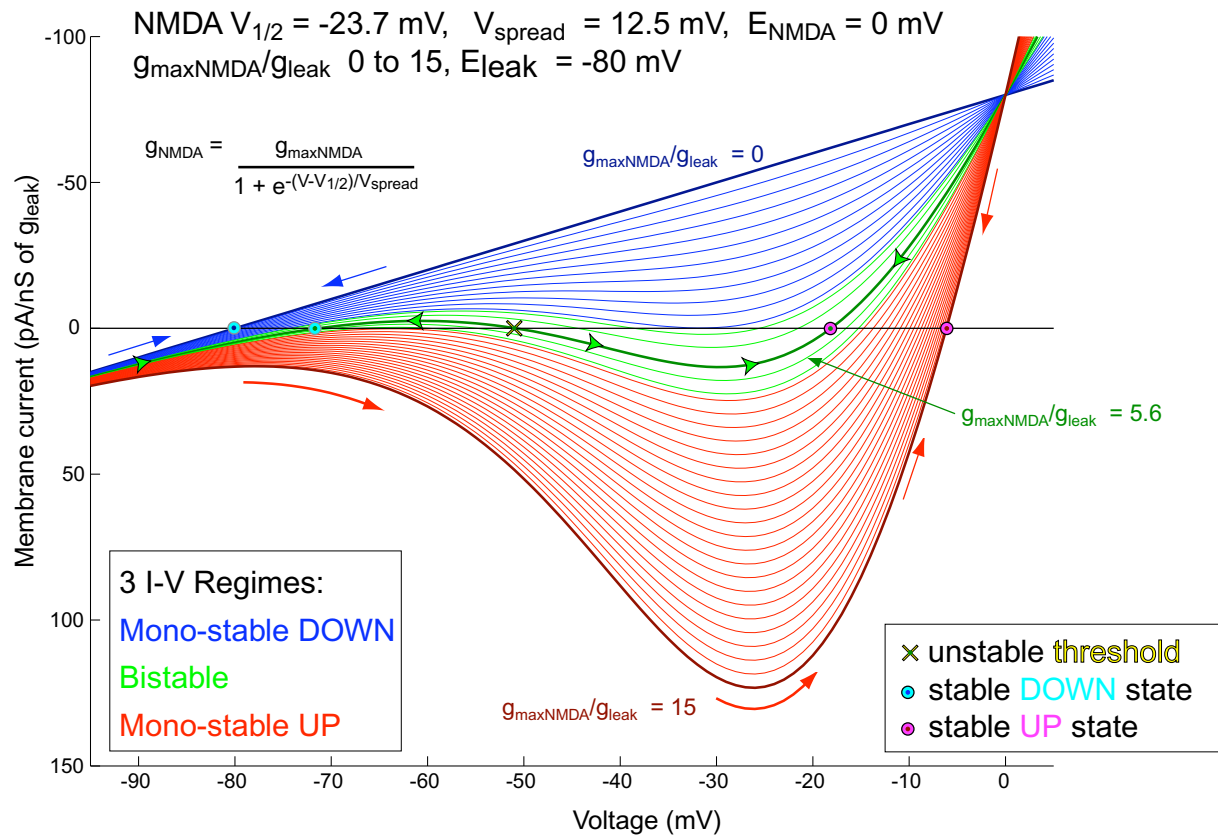
Stuart & Hausser
Nat. Neurosci. 4:63
(2001)

NMDA Spikes

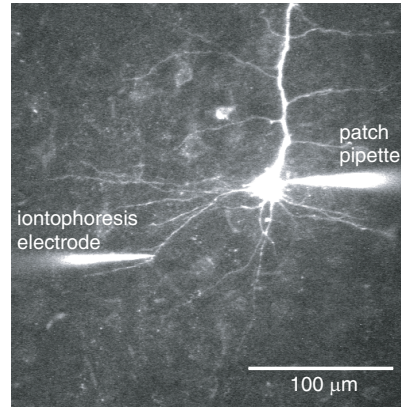
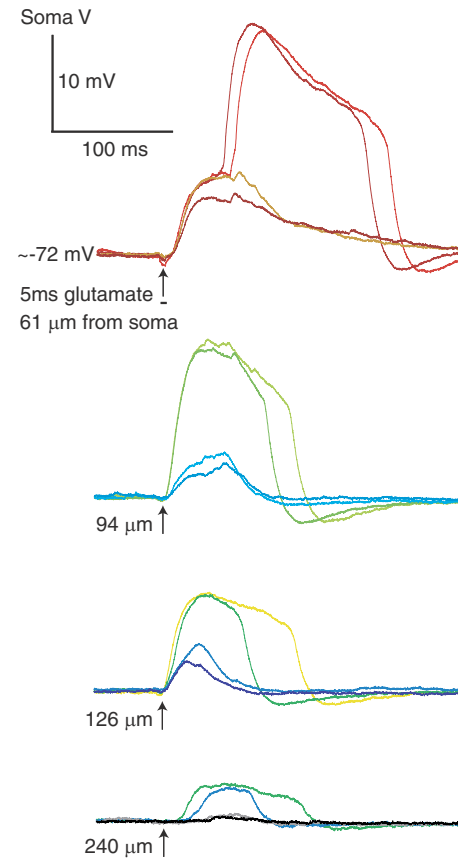
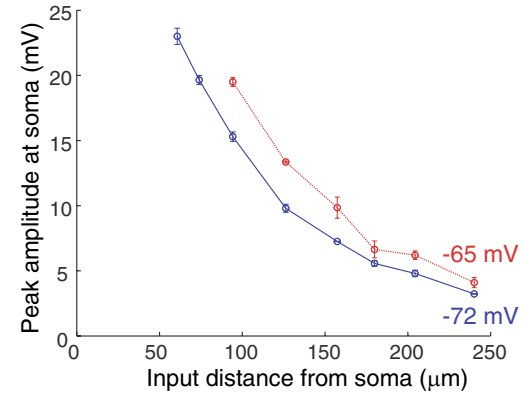
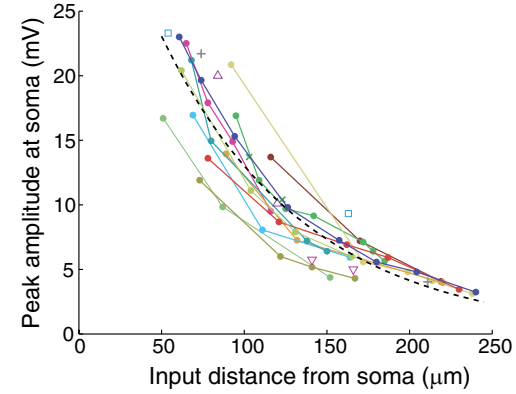
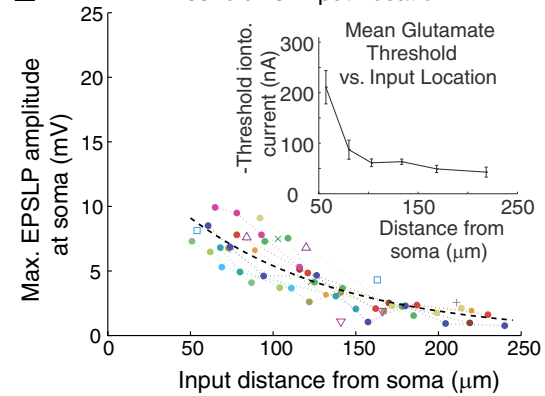


Schiller et al., Nature (2000)

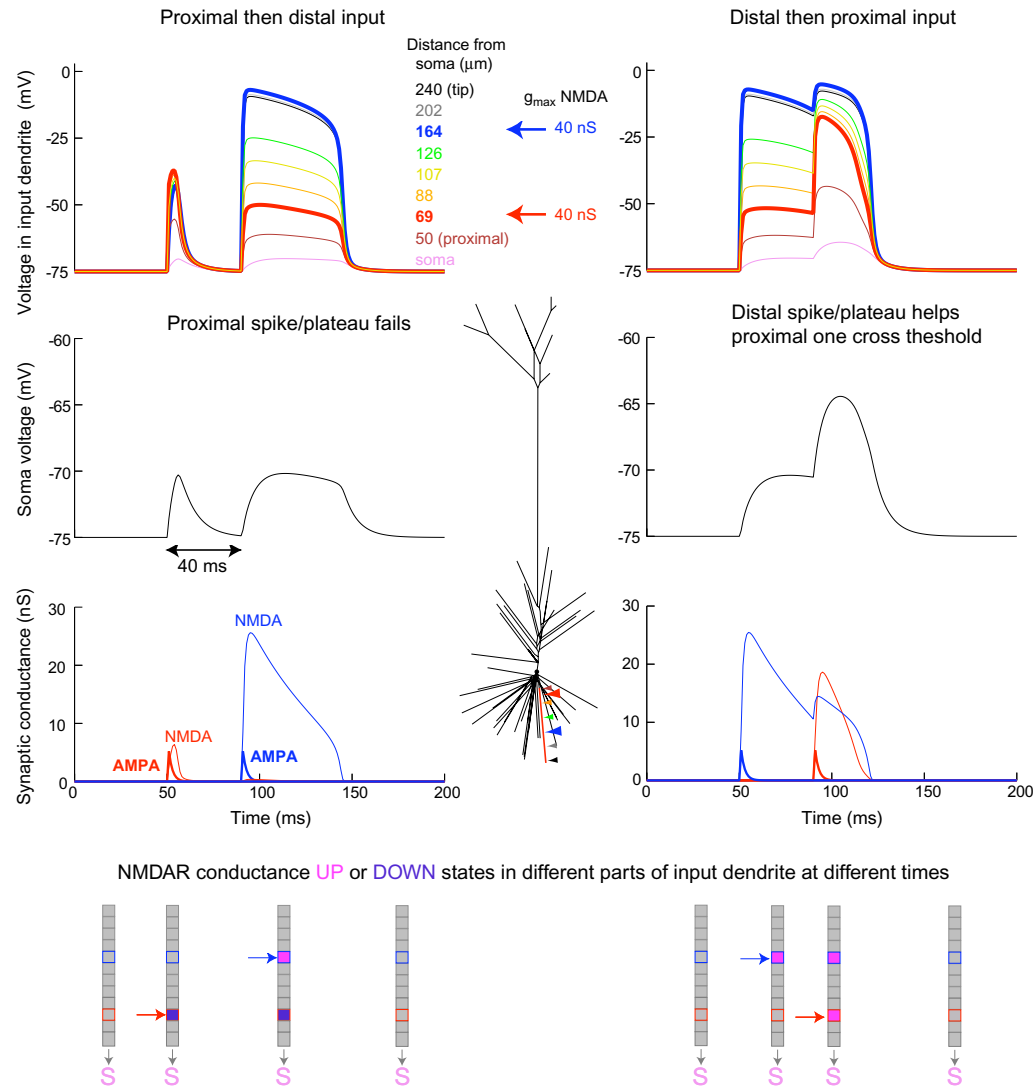
Families of NMDAR + Leak Single Compartment I-V curves



Supplementary Figure 4. Voltage-dependent NMDA conductance + passive leak can generate current-voltage (I-V) relations exhibiting 3 stability regimes. Theoretical illustration based on single compartment model with parameters indicated (Lisman et al. 1998). As the maximum (fully-depolarized) NMDA conductance g_{maxNMDA} increases, the I-V relation sweeps successively through three regimes: mono-stable DOWN ('boosting', blue lines), bistable (green lines), and mono-stable UP ('self-triggering', red lines), depending on the number and positions of the fixed points (zero current axis crossings). Stable fixed points on an exemplar I-V relation (thicker darker lines) for each regime indicated by concentric targets, unstable threshold fixed point on bistable exemplar marked by X. Neighboring I-V curves separated by increments in $g_{\text{maxNMDA}}/g_{\text{leak}}$ ratio of 0.2 (near regime boundaries), 0.4 (default) or 0.6 (just above bistable exemplar curve). Note negative currents are upwards (voltage clamp convention). System flow is indicated by arrows. For example, in the case of the thick dark green bistable curve, small negative voltage perturbations away from threshold result in negative currents through the membrane, hyperpolarizing the system progressively towards the stable DOWN state (cyan target). Small positive perturbations from threshold lead to positive currents, forcing the system to flow towards the UP-state (magenta target). Note that the DOWN and UP-states move to more depolarized levels as the NMDAR conductance increases, but the threshold is reduced. Pyramidal neurons typically exhibit inward rectification (see Supplementary Figure 2D3). The first segment of the I-V curve can be made steeper by including an inward rectification conductance in the membrane (not shown); this can make the N-shape more symmetrical as well as increasing the breadth (in parameter space) of the bistable regime.

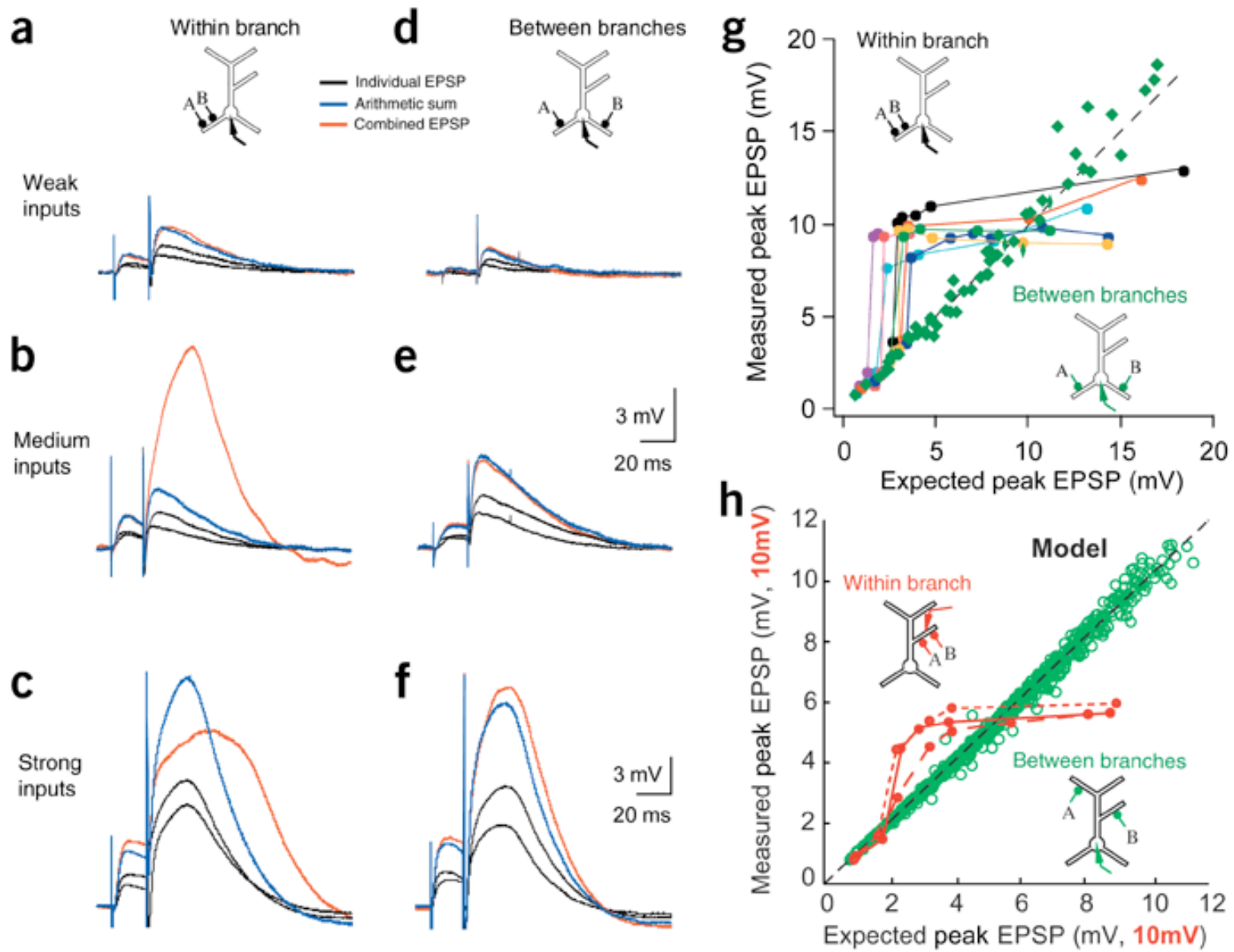
A Focal Glutamate Pulse to Basal Dendrite**B****C** Spike/plateau Amplitude vs. Input Location**D** Spike/plateau Amplitude vs. Input Location**E** Threshold vs. Input Location

Passive Compartmental Model with 2 Sequentially-activated Zones of NMDAR Conductance in a Single Basal dendrite

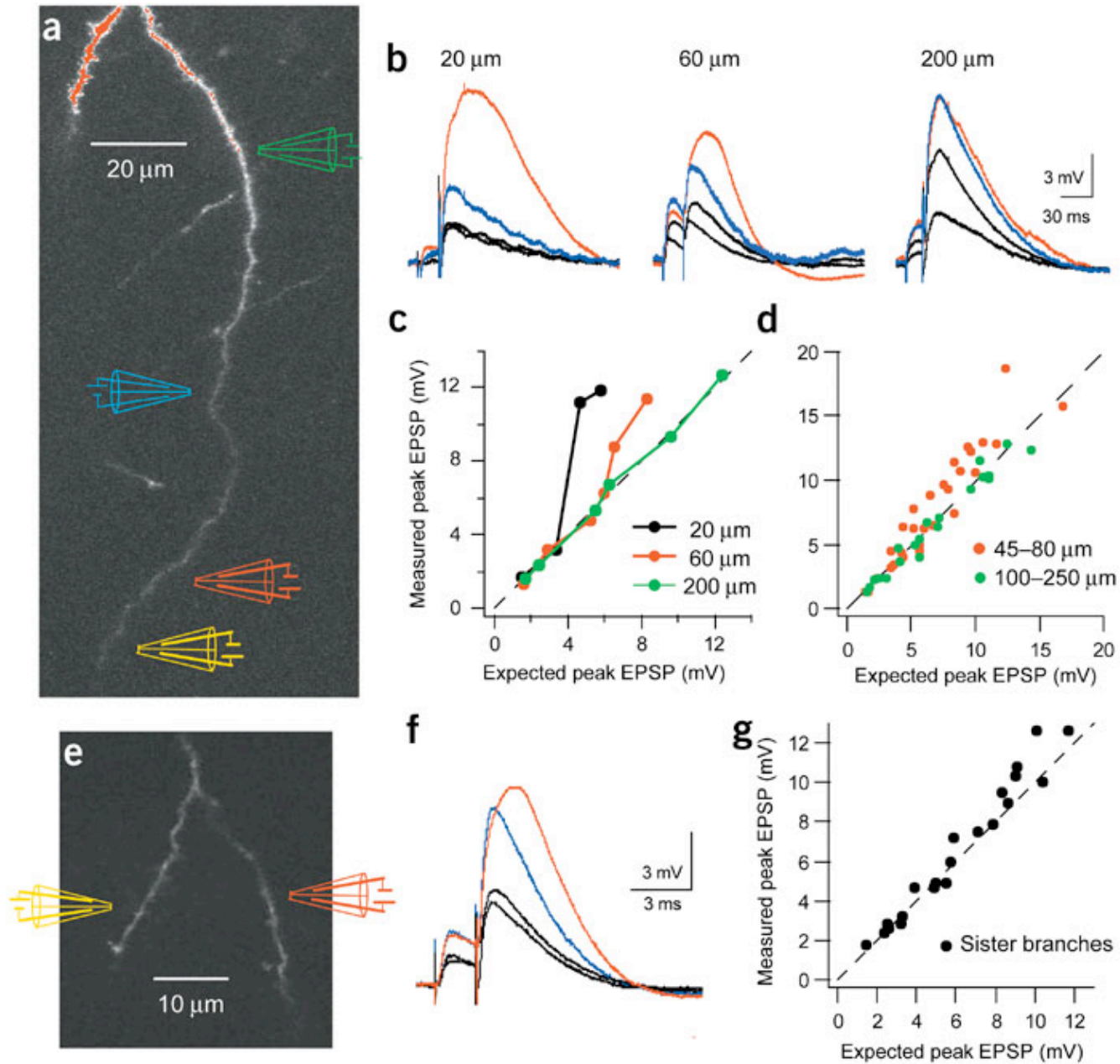


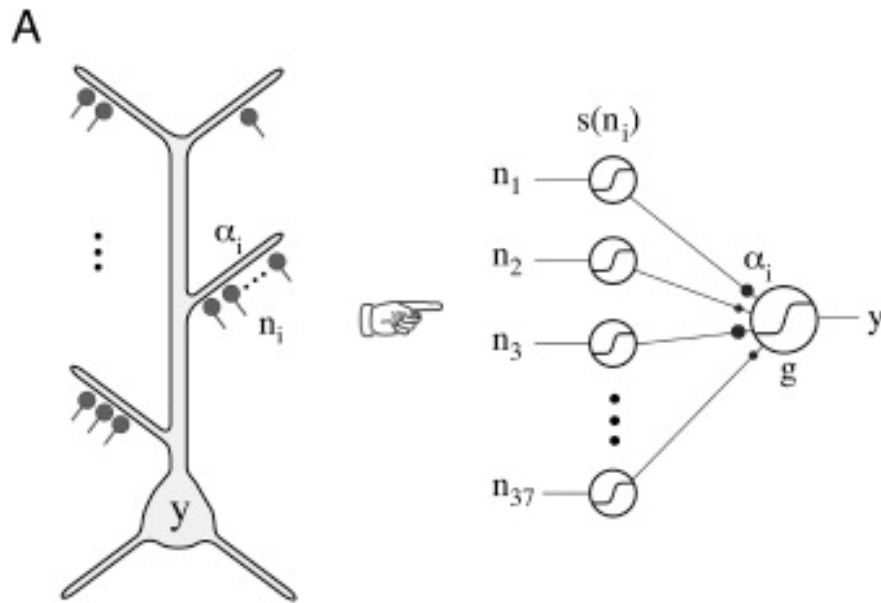
Supplementary Figure 6. Stimulating two different functional subunits in a single basal dendrite in a different temporal order can give dramatically different output. Same model as in Supplementary Figure 3, R_m 10000 Ωcm^2 , but with a 40 nS g_{max} NMDAR input at 164 μm and 69 μm at the indicated times. AMPAR component g_{max} is 6 nS at both sites. *Left:* proximal input followed after 40 ms by distal input. The proximal input fails to trigger an NMDA spike. The distal input then triggers a distal NMDA spike, but by then the proximal NMDAR conductance has decayed below the level at which it can produce an NMDA spike. *Right:* distal input followed by proximal input after 40 ms. The distal input is big enough to trigger a distal NMDA spike, in the subunit centered on 164 μm . The resulting depolarization propagates in attenuated form proximally, and lasts long enough to help the subsequent proximal input across threshold. The result is a proximal NMDA spike with a large somatic amplitude. *Lower panel:* schematic indicating which subunits are in high (UP) or low (DOWN) NMDAR conductance states at various times (magenta and dark purple, respectively).

Nonlinear Interactions and Functional Compartments



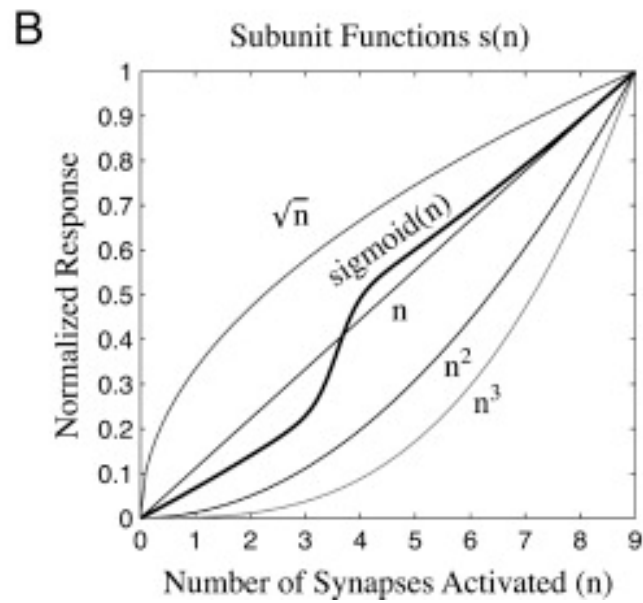
Estimating the Size of the Functional Unit





B. Mel

Two layer network model
of a pyramidal cell



Other Examples of Computation in Dendrites

Directional selectivity in starburst amacrine cell dendrites

Hausselet SE, Euler T, Detwiler PB, Denk W,
A dendrite-autonomous mechanism for direction selectivity in retinal
starburst amacrine cells. PLoS Biol. 2007 Jul;5(7):e185. Epub 2007 Jul 10.

Using nonlinear dendrites to build robustness into network models of persistent activity

Goldman MS, Levine JH, Major G, Tank DW, Seung HS,
Robust persistent neural activity in a model integrator with multiple
hysteretic dendrites per neuron. Cereb Cortex. 2003 Nov;13(11):1185-95.